NASA Technical Paper 1363

The NASA-Ames Research Center Stratospheric Aerosol Model

II. Sensitivity Studies and Comparison With Observations

O. B. Toon, R. P. Turco, P. Hamill,
C. S. Kiang, and R. C. Whitten

APRIL 1979

NASA

NASA Technical Paper 1363

The NASA-Ames Research Center Stratospheric Aerosol Model

II. Sensitivity Studies and Comparison With Observations

O. B. Toon
Ames Research Center, Moffett Field, California

R. P. Turco
R & D Associates, Marina del Rey, California

P. Hamill
Ames Research Center, Moffett Field, California

C. S. Kiang
National Center for Atmospheric Research, Boulder, Colorado

R. C. Whitten
Ames Research Center, Moffett Field, California

National Aeronautics
and Space Administration

**Scientific and Technical
Information Office**

1979

THE NASA-AMES RESEARCH CENTER STRATOSPHERIC AEROSOL MODEL

II. SENSITIVITY STUDIES AND COMPARISON WITH OBSERVATIONS

O. B. Toon
Ames Research Center

P. Hamill*
Ames Research Center

R. P. Turco
R and D Associates

C. S. Kiang†
National Center for Atmospheric Research

R. C. Whitten
Ames Research Center

SUMMARY

We have performed sensitivity tests on a one-dimensional, physical-chemical model of the unperturbed stratospheric aerosols and have compared model calculations with observations. The tests and comparisons suggest that coagulation controls the particle number mixing ratio, although the number of condensation nuclei at the tropopause and the diffusion coefficient at high altitudes are also important. The sulfate mass and large particle number ($r > 0.15$ μm) mixing ratios are controlled by growth, sedimentation, evaporation at high altitudes, and washout below the tropopause. The sulfur gas source strength and the aerosol residence time are much more important than the supply of condensation nuclei in establishing mass and large particle concentrations. The particle size is also controlled mainly by gas supply and residence time. OCS diffusion (not SO_2 diffusion) dominates the production of stratospheric H_2SO_4 particles during unperturbed times, although direct injection of SO_2 into the stratosphere could be significant if it normally occurs regularly by some transport mechanism. We suggest a number of *in situ* observations of the aerosols and laboratory measurements of aerosol parameters that can provide further information about the physics and chemistry of the stratosphere and the aerosols found there.

INTRODUCTION

Turco et al. (ref. 1) describe a sophisticated one-dimensional, physical-chemical aerosol model that simulates processes occurring in the Earth's stratosphere. In the following pages, the model's sensitivity to the physical and chemical processes, assumptions, and parameters contained in the model is explored; the model is used to illustrate the processes that are most significant for the various observed properties of the stratospheric aerosol layer; and new experimental and observational studies that might provide further insight into these significant processes are suggested.

---

*Now at Systems and Applied Sciences Corp., Hampton, Virginia 23666
†Now at the Georgia Institute of Technology, Atlanta, Georgia 30332

The next section describes a reference model that is later compared with other model runs containing altered physics (to perform sensitivity tests), as well as with observational data (to explore the physics of the stratospheric aerosols). The following sections illustrate the rates at which physical processes occur in the reference model and show the sensitivity of the model to the omission of various physical processes; demonstrate the sensitivity of the model to the values of variable or uncertain parameters that control the physical and chemical processes; and examine each of the commonly measured properties of the aerosols, relate the observations to the model physics, and suggest new observations.

Table 1 partially summarizes this work. The table indicates the sensitivity of each of the commonly observed properties of the stratospheric aerosols to each of the processes and parameters in the model. The sections of the paper that describe the sensitivity tests proceed through table 1 row-by-row because, by considering how all of the observable properties are affected by a given parameter, the maximum insight into the physics is obtained. Conversely, the section of the paper discussing observations proceeds through table 1 column-by-column. Since experimentalists only observe one parameter at a time, a consideration of all the processes affecting one observable should lead to a maximum understanding of the data.

REFERENCE MODEL DESCRIPTION

Reference 1 establishes a reference aerosol model that includes a well-defined set of physical and chemical processes and also includes specific choices for a number of naturally varying or uncertain parameters. We will compare reference model calculations of aerosol properties, observations of these properties, and model calculations of these properties using models in which some part of the physics or chemistry has been altered. If the variation between the reference model and the altered model calculation is larger than typical variations of observational data, then we can consider the model to be sensitive to the altered parameter. The comparisons also provide insight into the importance of the various physical processes for creating the observed aerosol properties.

The reference model contains chemical processes (described in ref. 1) and physical processes (described briefly in ref. 1 and more extensively by Hamill et al. (refs. 2, 3)). Sulfur-bearing gases are chemically converted to sulfuric acid vapor, causing a supersaturation of sulfuric acid at some altitudes. This vapor, along with water vapor, is then deposited onto inert "core" particles that originate in the troposphere and diffuse into the stratosphere. We refer to the bare core particles as condensation nuclei (Cn) or Aitken nuclei. The initial deposition of vapor onto Cn takes place by heteromolecular-heterogeneous nucleation. Subsequently, heteromolecular growth takes place as the particles grow into mixed sulfuric acid-water-core particles. Under certain conditions, which occur at high altitudes, the particles' environment may not be supersaturated and the particles thus evaporate. As the particles fall and diffuse, another growth process, referred to as water vapor growth, occurs because the ratio of acid to water in the particles is a function of the water vapor partial pressure and thus of altitude. Hence, as the particles move vertically they pick up or lose water molecules. The acid particles also undergo Brownian coagulation with each other and with Cn.

Although the reference model contains a large number of physical and chemical processes, it also omits some. For example, horizontal transport is not considered, and vertical transport is

parameterized by diffusion. The model Cn are assumed to be inert, whereas in the real atmosphere some Cn dissolve in H_2SO_4–H_2O solutions, altering the H_2SO_4 and H_2O vapor pressures (refs. 4, 5). We also ignore the possibility that Cn grow *in situ*. This growth process would be important if the cores were to constitute a significant portion of the aerosol, as some observations suggest (refs. 4-7). In our model, sulfuric acid is chemically formed in the vapor phase and then attached to the aerosols. We omit the possibility that gases, such as HSO_3, SO_3, or SO_2, react at the aerosol surface. New sulfuric acid particles in our model are always formed on preexisting Cn and we ignore homogeneous or ion nucleation. Observations show that the stratospheric aerosols always contain a nonacid portion (refs. 6 and 7, and Rosen, private communication), and theoretical studies support heterogeneous nucleation as the dominant form of nucleation (ref. 2). However, homogeneous, and more importantly, ion nucleation might be important under some circumstances. The elucidation of these omitted physical and chemical processes must await the development of more sophisticated aerosol models, as well as further observational and laboratory studies.

Each of the physical and chemical processes in our model contains adjustable parameters. Some are natural variables, such as temperature, water vapor partial pressure, sulfur gas concentration, and Cn concentration. Others are unknown or uncertain quantities, such as the H_2SO_4 vapor pressure, and the H_2SO_4 vapor sticking coefficient on aerosol droplets. The choice of the adjustable parameters in the reference model was *not* based upon "tuning" the model to fit observations of the stratospheric aerosols. Rather, the adjustable parameters were chosen to agree with other atmospheric or physical properties (ref. 1). For example, eddy diffusion coefficients were obtained from studies of gaseous tracers; and SO_2 and OCS abundances were based on observations, not on a desire to obtain a specific stratospheric aerosol mass. Uncertain parameters were set to limiting or most probable values based upon laboratory and theoretical studies.

To interpret properly the sensitivity tests described in the next two sections, the reader should be familiar with the observed variability of the stratospheric aerosol properties and should be aware of how well the reference model compares with observations. Figure 1 compares typical data with reference model calculations of five commonly observed parameters: number mixing ratio of all particles (total particle mixing ratio); number mixing ratio of particles with radius larger than 0.15 μm (large particle mixing ratio); mass mixing ratio of sulfate; ratio of the concentration of particles larger than 0.15 μm to the concentration of particles larger than 0.25 μm (particle size ratio); and particle size distribution. We shall discuss these observations at greater length in a later section.

MODEL SENSITIVITY TO PHYSICAL PROCESSES

The reference model contains a number of physical processes that control the size, number, and distribution of the aerosols: nucleation, growth, evaporation, coagulation, diffusion, and sedimentation. We will consider the relative importance of these processes first by intercomparing their rates in the reference model and, second, by examining the model calculations of four "observables," using a sequence of models in which each physical process is omitted in turn.

Rates of Physical Processes

Figures 2(a) through 2(c) show the rates of the physical processes in the reference model as functions of altitude and particle size. The ordinates of these figures represent the fraction of the number of acid droplets of a given volume and altitude that are created (solid lines) or destroyed (dashed lines) every second. Since our model separates the particles by radius and altitude into a number of bins, this structure influences the interpretations of the rates. The bin sizes increase geometrically by factors of 2 in volume and arithmetically by 2-km increments in altitude. Thus, the rates are the inverse of the time required for all the particles in a bin to double in volume or to move 2 km in altitude. Because there are very few large particles compared to small ones (fig. 1(e)), the rates of production or loss of *single* particles in bins of different sizes differ by much larger factors than do the rates for emptying or filling an entire bin. We have chosen to consider the rates at altitudes of 16, 20, and 30 km because all three are in the aerosol layer; 16 km is just above the model tropopause (13 km), 30 km is just below the model evaporation level (33 km), and 20 km is well-removed from both boundaries and is also the typical height at which observations have been made.

Aerosol droplets can only be produced by nucleation. Even so, few particles at most altitudes and sizes originate by nucleation of bare cores mixed up from the troposphere or down from the evaporation level. Particles in the smallest size bin at 16 and 30 km are the only ones generated predominantly by nucleation. At 20 km, even the particles in the first size bin are produced mostly by diffusion of acid particles from higher and lower altitudes, which are closer to sources of unnucleated particles. Nucleation becomes relatively more important at 16 km for larger particles because the size distribution of acid aerosol at 16 km is so steep at very large sizes that the number of the larger tropospheric Cn diffusing to 16 km is comparable to the number of the large acid particles. Because few large cores ascend to 30 km as a result of sedimentation losses, the up-turn of the nucleation rate at large sizes does not occur in the 30-km rates. In reality, meteoritic debris or rocket exhaust (ref. 18) might provide a large particle source at high altitude.

Diffusion and sedimentation are numerically combined in our model to reduce artificial numerical diffusion and in figure 2 we refer to the combination as transport. Transport is a source of small particles at all three altitudes, but it is dominant at 20 km only. Of course, just at the tropopause and at the evaporation level, transport is a sink for small acid particles. In our model, small core particles cross the tropopause or evaporation level and quickly nucleate. They then diffuse to the other stratospheric altitudes. Because there is no other source of small droplets in our model, transport is necessarily a net source of small acid particles throughout most of the model stratosphere.

Transport is the dominant loss process at all altitudes for particles larger than 0.1 to 0.3 μm. The increasing importance of transport with particle size is partly due to the growing importance of sedimentation. Particles with radii greater than 1.0 μm have fall times that are short compared with the typically observed residence times of stratospheric tracers. The transport rate due to diffusion is influenced by the vertical mixing ratio gradients. Figures 1(a) and 1(b) show that the mixing ratio profile for large particles has a stratospheric maximum, but the profile for small particles continually decreases with increasing altitude. This accounts for much of the size-dependence of the transport loss curves shown in figures 2(a) through 2(c). For example, at 20 km the altitude profile of the mixing ratio is a strong function of size. Particles of size 0.1 μm have nearly constant mixing

ratios and thus small diffusion loss, but slightly bigger particles have a maximum mixing ratio near 20 km so that they have larger diffusion loss.

Water vapor growth occurs when a particle of given acid-water concentration moves vertically to a region with a water vapor partial pressure that is not in equilibrium with the particle's composition. Then the particle must quickly shrink or swell, changing its water content to reach equilibrium. Although water vapor growth is not an important loss mechanism at any altitude, it is the dominant growth process at 20 km for particles larger than 0.5 μm. In our reference model, the particle volume increases by about 50% due to water growth, as particles created near 30 km fall to 20 km. Thus, particles cannot grow across even a single bin by falling from 30 to 20 km so that the loss rate due to this process is small. However, for large particles, the size distribution is very steep. Relative to the number of particles in a bin, there are great numbers of particles just across the lower bin boundary and these can grow into the next bin and greatly increase the concentration. Hence, the gain due to this process is significant for large particles.

Growth due to heteromolecular condensation of water vapor and H_2SO_4 molecules is a mechanism coupling particles of different sizes at a single altitude. Growth can be both a sink and a source of particles of fixed size. In a given bin, particles are created from smaller sizes as they enter the bin and are lost to larger sizes as they leave the bin. The size-dependence of the growth rates in figure 2 is partly due to the dependence of the vapor condensation rate on particle radius and is partly due to the steepness of the size distribution at large sizes, as discussed in reference 1. The rate of gain by growth exceeds the rate of loss by growth except for particles in the smallest bin (the first bin has no source of smaller particles). Growth also dominates all other gain processes except for very large particles that are created by nucleation, coagulation, or water vapor growth. At high altitudes, growth is the dominant, small-particle loss process because there are not enough particles available for coagulation to be efficient.

The final physical process contained in our model is coagulation, which may be a sink for small particles as they coagulate to form larger ones, or a source as smaller particles coagulate to produce particles of the size being considered. The coagulation loss rate declines steadily with increasing size. Small particles can collide with many larger particles, removing the small particles from their initial bin. Large particles have few larger particles available for collisions and the smaller particles with which they do collide often do not carry enough volume for the resulting particle to be in a larger size bin. The coagulation gain rate, on the other hand, is nearly independent of size or increases with size. Because the size distribution is steep, at larger sizes there are more particles in the preceding bins relative to the number of particles in a bin. The coagulation kernels between adjacent bins are nearly independent of size, while the kernels between large and small particles increase with size. Thus, the potential for creating new coagulated particles grows with particle size. An additional important factor for large sizes is the direct addition to a bin of unnucleated core particles as a result of coagulation with small acid particles. Whenever the Cn size distribution introduces numbers of particles comparable to the acid particle numbers, then such a process can create particles by this "coagulation-nucleation" process. Of course, even though such particles may be barely wet, they are counted as droplets.

The coagulation rate depends on the square of the particle number concentration. For this reason, coagulation is not an important process at 30 km, where the particle concentrations are small (fig. 1(a)). Coagulation is not the dominant particle production process at any size except for large particles near the tropopause for which the coagulation-nucleation process makes

coagulation appear to be important. For particle sizes near 0.1 μm, coagulation is a moderately important production mechanism at 16 and 20 km, but coagulation is quite an important small particle sink mechanism at 16 and 20 km. Since growth losses are more than compensated by growth gains, coagulation is the means by which most small particles (<0.2 μm) are lost at these altitudes.

Sensitivity to Physical Processes

In the preceding paragraphs the rates of various mechanisms in the reference model were examined and we found that nucleation, transport, water vapor growth, heteromolecular growth, and coagulation are each a dominant loss or gain mechanism at some size or altitude. Thus, no model can be complete without including all these processes. We will now reexamine their importance by presenting calculations in which one or another of these processes has been omitted. The sensitivity calculations were performed using the same initial conditions as used for the reference model.

Figures 3(a) through 3(d) compare the results of reference model calculations of four observables – total particle number mixing ratio, large particle number mixing ratio, mass mixing ratio, and particle size ratio – with model calculations in which growth, coagulation, water vapor growth, and sedimentation have been omitted. Of course, the omission of nucleation would produce results similar to those obtained by omitting growth. Omitting diffusion also suppresses the layer since no gases or nuclei will enter the stratosphere. The reader may recall that the reference model is compared with observations in figure 1.

Removing sedimentation from the reference model causes the total particle mixing ratio above 24 km to be nearly constant, but it does not alter the mixing ratio below 24 km (fig. 3(a)). Thus, sedimentation is the dominant total particle sink above 24 km. Its increasing importance with altitude is due to the increasing mean free path of air, which yields a steady increase in particle fall velocity. Removing sedimentation from our model has a more dramatic effect on large particle (fig. 3(b)) and mass (fig. 3(c)) mixing ratios than on the total particle mixing ratio because large particle and mass mixing ratios are dominated by big particles and the sedimentation velocity increases with particle radius. The particle size ratio (fig. 3(d)) decreases if sedimentation is removed because larger particles no longer fall faster than smaller ones.

Omitting water vapor growth from the reference model causes almost no change in the calculated results. The four "observables" are not very sensitive to particles whose size exceeds 0.5 μm, and figure 2 suggests that water growth is only important for quite large particles. For example, omitting water vapor growth leads to two orders of magnitude decrease in the number of particles in the largest size bin ($\sim$2.5 μm) at 20 km.

Omitting all growth from our reference model produces a small increase in the total number of particles. Omitting growth decreases the total particle mass, thereby reducing the sedimentation rate, and decreases the total particle surface area, thereby reducing the coagulation rate. Growth itself cannot change the total number of particles. It is only because of the coupling to these other processes that a change occurs when growth is omitted. Of course, growth does directly affect the number of large particles and the total mass mixing ratio. The small residual layer remaining in the no-growth case is mainly a remnant of the initial conditions remaining after 5 years of simulated

model decay of the layer. Of course, growth strongly affects the particle size ratio, which, in the absence of growth, is determined by the assumed tropospheric core size distribution as modified by coagulation and sedimentation.

Martell (ref. 19) has suggested that the stratospheric large particle layer is not created by the chemical conversion of sulfur-bearing gases and the growth of aerosol sulfates in the stratosphere, but rather that tropospheric sulfate particles of very small size mix into the stratosphere and coagulate to produce the observed layer. Further, he presented arguments suggesting that the sulfate mass mixing ratio peaks in the troposphere. Current data show on the contrary that the sulfate mass mixing ratio actually peaks in the stratosphere. Coagulation conserves mass and could not create a mass mixing ratio peak in the stratosphere. Thus, the new data rules our Martell's idea. However, to test Martell's hypothesis we show the results of a calculation in figure 3 with growth omitted but with enhanced numbers of tropospheric Cn (reference model X 10) and a less steep size distribution to enhance the mass. These changes prevent the calculation from being dominated by initial conditions, yield reasonable particle numbers and masses in the stratosphere, and create a mass mixing ratio peak in the troposphere, as Martell desired. However, the results in figure 3(b) show that the large particles do not form a well-defined layer. We therefore conclude that Martell's suggestion does not appear to be viable. We have not explored exotic variations of other parameters, such as diffusion profiles, or perhaps a two-dimensional model with strong horizontal mixing which could yield isolated cases where a layered, large-particle structure would appear.

Another piece of evidence concerning the importance of growth is the study by Castleman et al. (ref. 20) of sulfate and its isotopic ratio after several volcanic eruptions. Following an eruption, they found a delay (longer than typical transport times) of the sulfate mass buildup and, in addition, a slow but uniform change in the isotope ratio. These observations are consistent with slow *in situ* gas-to-particle conversion, rather than with production of stratospheric particles by coagulation from particles formed in the volcanic plume at the time of the eruption.

The final process examined in figure 3 is coagulation. Removing the coagulation process dramatically increases the total particle mixing ratio which, except for sedimentation effects, becomes constant with altitude. Coagulation is clearly the dominant total number (hence small particle) loss process. Coagulation removal also has an effect on the large particle mixing ratio, the mass mixing ratio, and the particle size ratio, all of which seems to suggest that coagulation is an important loss process for particles larger than 0.1 μm. Simply omitting coagulation leads to a large increase in the total number of particles, which increases the particle surface area, and forces growth to occur on more, smaller, particles. Since the average particle size is decreased, sedimentation is decreased, enhancing particle numbers at high altitudes. Also, the acid mass is redistributed from large to small particles enhancing the size ratio. To better define the role of coagulation we therefore performed another calculation omitting coagulation, but in this calculation we reduced the number of Cn particles at the tropopause by a factor of 10 so that the number of particles at 20 km was comparable to the number in the reference model. Figures 3(b) through 3(d) show that coagulation has a small effect on mass mixing ratio, large particle mixing ratio, or the particle size ratio once the basic total number of particles has been reduced to the observed values.

MODEL SENSITIVITY TO ADJUSTABLE PARAMETERS

Each of the physical processes just discussed contains a number of variable or uncertain parameters whose values can be adjusted. We may group these into parameters that control the sink or source of gases; parameters that control the residence time of particles and the sinks and sources of cores; parameters that control the nucleation rate; and parameters that control the particle growth rate. Sedimentation and coagulation in our model do not explicitly contain any adjustable parameters except for a relatively weak temperature dependence. In the following pages we will explore the model's sensitivity to several adjustable parameters by comparing the results of reference model calculations of four commonly observed quantities with the results of calculations performed using reasonable variations of the adjustable parameters.

Parameters Controlling Sinks and Sources of Gases

Figures 4(a) through 4(d) present the results of calculations made with altered supplies of sulfur-bearing gases. The reference model contains OCS and SO_2, which diffuse into the stratosphere from the troposphere. The latter reacts with OH just above the tropopause, but OCS must be transported to higher altitudes (between 25 and 30 km) before it can be photolyzed. Another potential source of SO_2, not contained in the reference model, is direct stratospheric injection. Injection might be due to a volcanic eruption, high-flying aircraft, or large-scale mixing processes. Because a one-dimensional model is not well-suited for considering stratospheric injection processes, we have modeled two simple injection situations: in one, SO_2 is injected over an 8-km-thick layer just above the tropopause; in the other, the injection is confined to a 2-km-thick layer centered at 20 km. For the injection calculations, we removed the SO_2 and OCS diffusion sources and adjusted the SO_2 injection rate to provide enough sulfur to agree with observed rates of natural aerosol mass removal from the stratosphere (refs. 15, 21). We also experimented with increased SO_2 and OCS concentrations in the troposphere. Several measurements of ground level OCS have been made showing that it is a ubiquitous substance with a nearly constant mixing ratio (refs. 22, 23). We increased OCS by a factor of 5 to represent a hypothetical increase in its concentration due to increased production. SO_2 is highly variable in the troposphere, and only one measurement has been made at the tropopause (ref. 24). Hence, we have examined a case with 10 times the reference SO_2 as a possible upper bound due to variability and possible future increases from accelerated emission.

Figure 4(a) shows that the total particle mixing ratio is nearly independent of the gas source strength. The changes at high altitude occur because an increased source strength yields larger particles that coagulate and fall faster while a decreased source strength produces the opposite effect. By contrast, the mass mixing ratio, large particle mixing ratio, and particle size ratio are all strongly affected by source strength. Removing OCS altogether leads to a marked decrease in the sulfate mass and large particle concentrations in the layer. It also moves their maximum mixing ratio values to lower altitudes near the level where SO_2 is converted to H_2SO_4, and it changes the particle size ratio dramatically. Removing the SO_2, on the other hand, produces only a slight change in the layer characteristics. Increasing the OCS and SO_2 abundances at the tropopause by factors of 5 and 10, respectively, does increase the large particle and mass mixing ratios over those in the reference model, but not nearly by the factors of 5 or 10. When we compare the 5 $\times$ OCS and 10 $\times$ SO_2 calculations with those for which SO_2 or OCS, respectively, are absent, the mixing ratio

increases are still less than factors of 5 or 10. One interesting point is that the SO_2 increase has a more noticeable effect on the mixing ratio of large particles, and the OCS increase has a more noticeable effect on the aerosol sulfate mass mixing ratio. This may be due to the difference in the altitude of the two sources. SO_2 is converted to H_2SO_4 at low altitudes in a region containing many small particles, which quickly grow to sizes near 0.1 μm. However, there are few small particles at 25 to 30 km where OCS is oxidized to H_2SO_4 so that the OCS increase has less potential for producing many large particles. It is significant that we are discussing mixing ratios here, for the increase in the total column *number* of large particles in the stratosphere is even greater in the augmented SO_2 case than the OCS case. The mass mixing ratio is enhanced more by the OCS partly because it requires less absolute mass addition to double the mass mixing ratio at 30 km (where OCS is oxidized) than at 20 km, but also because 30 km is further from the tropospheric sink so that the residence times there are longer.

An increase in the supply of SO_2 or OCS molecules ought to lead to an increase in the H_2SO_4 vapor concentration and thereby to an increase in the H_2SO_4 supersaturation ratio S, which is the ratio of H_2SO_4 partial pressure in the atmosphere to the H_2SO_4 vapor pressure P_v. The quantity $P_v(S - 1)$ controls the aerosol growth rate. Figure 5 compares the reference model supersaturation to the supersaturation with no OCS, with 10 X SO_2 and with 5 X OCS. Evidently, a change in the supply of sulfur gas leads to change in particle surface area, which alters the growth rate in a manner that compensates for the gas supply change. This compensation prevents the partial pressure of H_2SO_4 from increasing to its maximum possible value, and the supersaturation remains nearly constant. The H_2SO_4 supersaturation is also an important parameter controlling homogeneous and ion particle nucleation rates. Thus, for moderate steady-state changes in sulfur gas supplies, homogeneous nucleation is no more likely to occur than it is in the reference case. Of course, large, nonsteady-state perturbations will not have constant supersaturation.

If we inject SO_2 directly, rather than allowing OCS or SO_2 to diffuse into the stratosphere, we find that the layer profile is not greatly modified. In this case, mixing ratio peaks are located just above the highest altitude of injection. Moreover, injection close to the tropopause level is less efficient for producing large particles than injection at 20 km, because of the shorter particle and gas residence times at these lower altitudes.

The SO_2 and OCS sources just considered produce H_2SO_4 vapor, which then attaches itself to the aerosol particles. However, the chemistry leading to H_2SO_4 production probably yields sizable quantities of the intermediate radical HSO_3, which might also condense on aerosols and thus short-circuit the H_2SO_4 growth process. As is shown in figure 5 of reference 1, the predicted concentration of HSO_3 exceeds that of H_2SO_4 at 20 km in the reference model because H_2SO_4 has a strong aerosol sink near 20 km. If HSO_3 is allowed to interact directly with particles, the gas phase concentrations of HSO_3 and H_2SO_4 are altered. However, the aerosol properties remain unchanged (figs. 4(a)-4(d)). This is one example of an important property of our model: the aerosol properties are fixed primarily by the *total* sulfur supply and the residence time.

Another parameter that controls the gas sources and sinks is the OH abundance. OH is a reactant in the rate-controlling reaction step for the conversion of SO_2 into H_2SO_4. OH is not calculated interactively in our reference model, although it is certainly variable in reality and will change with large perturbations of the layer. Calculations using a more complete chemical model show that OH is not affected by sulfur chemistry in the unperturbed aerosol layer being considered

here (see ref. 1). Moreover, as we will show later (figs. 9(a)-9(d)), a factor of 3 change in the OH abundance does not strongly affect the stratosphere aerosol properties in the model.

Parameters Controlling Particle Residence Time and Supply of Cores

A nonacid core is essential for the formation of stratospheric aerosols in our model. These can originate as very small Cn in the troposphere and then be mixed to higher altitudes. As shown in figure 1(a), our assumed concentration of Cn at the tropopause is in good agreement with observed values of about 300 particles/cm^3. The limited observations of this quantity (fig. 1(a)) suggest that it may vary by factors of ±2 at the tropopause. Hence, to encompass most possible long-term variations of the concentration, we have examined changes of an order of a factor of ±5 in the number of Cn at the tropopause (figs. 6(a)-6(d)). The Cn at the tropopause also have a specific size distribution. In the reference model we assume the Cn size distribution varies as r^{-4}. To our knowledge there are no complete measurements of the size distribution in the upper troposphere. The choice of an r^{-4} size distribution yields both a reasonable total number (fig. 1(a)) and a reasonable mass mixing ratio (fig. 1(c)) of Cn at the tropopause; however, the r^{-4} distribution has slightly too few 0.1 μm particles compared to the total (fig. 1(b)). Accordingly, in figures 6(a) through 6(d) we have tested two alternative size distributions: one is an r^{-3} distribution, which contains much more mass, as well as many more large particles; the other is monodispersed at 0.01 μm (these are the smallest size particles possible in our model). In each case, the Cn distribution is adjusted so that the total number of particles at the tropopause is about the same in the altered cases as in the reference model. Although other size distributions are possible, we have merely taken the simplest possible cases for our study. However, as discussed below, we do not believe that the model is sensitive to the Cn size distribution as long as the total Cn mass is not excessive.

Figure 6(a) shows that changing the Cn concentration by a factor of 5 or 1/5 at the tropopause only results in factor-of-2 changes in the total particle mixing ratio at higher altitudes. Coagulation is strongly nonlinear in the particle concentration, so it is relatively difficult to alter the total number of stratospheric particles. Of course, the particle concentration is nearly independent of the Cn size distribution because most Cn are too small for sedimentation to affect the vertical profile.

A factor of 5 change in the Cn concentration results in a change in the large particle mixing ratio (~25% at 20 km) that is barely significant compared to the observed variability, and it results in an even less significant change in the aerosol mass (figs. 6(b) and 6(c)). Of course, adding (subtracting) Cn produces more (fewer) small particles and the particle size ratio increases (decreases). The fact that the aerosol mass and the number of large particles do not double when the number of cores is doubled is quite significant. It implies that in our model the net mass deposited on stratospheric particles is controlled by the rate of chemical production of H_2SO_4 and by the mean residence time of aerosols. The rate of deposition of acid vapor onto the particles is not the time-limiting step however, for if it were, increasing the number of Cn would greatly increase the aerosol mass.

Altering the size distribution of the Cn has little effect on the aerosol layer properties. The number of large particles at 20 km is enhanced by 20% using the r^{-3} distribution, but the change is quite small considering the order of magnitude difference in the number of large particles at the tropopause between an r^{-3} and r^{-4} size distribution. The mass of the layer is strongly affected by the r^{-3} distribution only because the cores themselves contain considerable mass.

One curiosity of the monodispersed core calculations is that the particle size ratio is slightly smaller than in the reference model (fig. 6(d)). Apparently, this effect occurs because very large particles are not easily produced in the monodispersed case, so that their acid mass is redistributed to particles of size near 0.1 μm, flattening the size distribution in that size region.

Another parameter that affects the aerosols near the tropopause is the assumed tropospheric rainout rate. If acid particles fall or diffuse out of the stratosphere, they must still be removed from the upper troposphere, and the rate-controlling process in our model is rainout. Martell and Moore (ref. 25) and Moore et al. (ref. 26) discussed the available evidence concerning tropospheric aerosol removal rates and concluded that residence times in the troposphere are 1 week or less. Our reference model profile of the rainout rate yields a mean residence time of several days in the troposphere, with 1 day being the value at the ground and 7 days the value at 12 km.

Some older studies (see refs. 25 and 26) suggested tropospheric aerosol residence times averaging nearly 1 month. We have simulated these longer times by multiplying the residence time profile in our reference model by a factor of 14. Figures 6(a) through 6(d) show that with a longer residence time the mass mixing ratio and the large particle mixing ratio increase near the tropopause. These changes are due to the decreased strength of the tropospheric sink. Of course, the particle size ratio decreases since large stratospheric particles have a longer time to grow in the stratosphere and are not removed as rapidly just below the tropopause.

A parameter closely related to the tropospheric rainout rate (at least in its function in our model) is the fraction of the tropospheric particles that is composed of sulfuric acid solution. Figure 5 indicates that the H_2SO_4 supersaturation is large just below the tropopause, suggesting that H_2SO_4 particles could form there, and of course H_2SO_4 particles are commonly observed at ground level (e.g., refs. 27, 28). We have not attempted to model tropospheric aerosols and so we have set the core nucleation rates in the troposphere to zero despite the high supersaturation. Our motivation was to avoid confusing our stratospheric calculations with questions about tropospheric particles. In figures 6(a) through 6(d), we show that including the nucleation of tropospheric particles in the reference model produces only very small changes in our stratospheric observables. The particle size ratio in the troposphere is increased, however, due to the nucleation and growth of Cn.

The reference model results are not sensitive to the presence of tropospheric sulfuric acid particles because the residence time in the upper troposphere is so short that only a few of the new particles have time to grow and eventually diffuse into the stratosphere. In figures 6(a) through 6(d) we have also presented a calculation with a residence time that is four times that in the reference model and with nucleation of sulfuric acid aerosols in the troposphere. Interestingly, the layer is now modified slightly (<25%) at all altitudes, due not only to the decreased strength of the tropospheric large particle and mass sinks, but also to the increased size of the Cn particles diffusing upward from the troposphere. We chose this moderate residence time (equivalent to a mean residence time of about 1 week) because it is probably an upper bound consistent with modern views (ref. 26). Note, however, that the growing Cn in the troposphere produces there a very large value of the particle size ratio parameter (fig. 6(d)) compared with typical observed values (fig. 1(d)).

As we discussed previously, the H_2SO_4 supersaturation is very large below the model tropopause. Figure 5 shows that simply allowing particles to nucleate in the reference model

troposphere does not substantially decrease the supersaturation. As the aerosol residence time increases to 4 days, however, the supersaturation does decrease, but the supersaturation still remains 10^4 at 12 km.

Another parameter affecting the interaction of stratospheric and tropospheric aerosols is the tropopause height. The tropopause height varies with latitude, and has seasonal and random fluctuations at any given location as well. Figures 7(a) through 7(d) illustrate calculations in which the tropopause has been moved from the reference model height of 13 km to 9 km and 17 km. The movement is accomplished by changing the reference model diffusion coefficient profile so that the break at the tropopause occurs at different altitudes (fig. 8) and by changing the nucleation pattern so that particles below the new tropopause level are not nucleated. The total particle mixing ratio is strongly modified by changing the tropopause height. The higher tropopause calculation has fewer total particles (but the same mixing ratio) at the tropopause than the lower tropopause calculation. However, due to the rapid rate of coagulation compared with local residence times for particles, the lower tropopause case has many fewer particles at the same stratospheric altitude as the higher tropopause case. Just the opposite situation occurs for the large particle and mass mixing ratios. The lower tropopause case has higher mixing ratios and a smaller particle size ratio because the aerosol residence time at a fixed height is increased so that more growth can take place and because the diffusion of OCS and SO_2 is enhanced by increased concentrations at the tropopause level.

The diffusion coefficient profile used in our reference model is a modified Wofsy-McElroy profile (ref. 29). Two other eddy diffusion profiles are used in stratospheric chemical models: one proposed by Hunten (ref. 30) and one attributed to Dickinson and Chang (ref. 31). As illustrated in figure 8, the Hunten profile has noticeably smaller diffusion coefficients at high altitudes than the reference model, and the Dickinson-Chang profile is much less abrupt at the tropopause than the reference model profile. We have performed calculations with these alternative profiles, modified slightly below 8 km so that they have the same diffusion coefficient as our standard profile at low altitudes.

Figure 7(a) shows that a calculation using the Hunten profile yields many fewer particles at high altitudes than does the reference model because, with the smaller diffusion coefficients, sedimentation dominates vertical transport. The Dickinson-Chang profile yields a total particle mixing ratio similar to that of the reference model at high altitudes, but the mixing ratio falls off less strongly than that of the reference model near the tropopause. The large particle and mass mixing ratios are both decreased with either of the alternative diffusion coefficients, apparently due to decreased diffusive supplies of sulfur-bearing gases. The smaller diffusion coefficients of the Hunten profile do not bring as much OCS to high altitudes so fewer large particles are made than in the reference model; and of course the large particles are more rapidly removed by sedimentation. Also, the aerosol growth is decreased because the slower diffusion below the tropopause allows less SO_2 to reach the stratosphere before it is washed out or chemically converted to H_2SO_4. The Dickinson-Chang diffusion profile yields a shorter residence time for gases and particles just above the tropopause and a longer residence time in the troposphere; as a result, the particles have less chance to grow just above the tropopause, and SO_2 transported upward from the troposphere is almost completely removed before it reaches 14 km. The Dickinson-Chang profile does not suppress the OCS, however, so the higher altitude part of the layer closely resembles the reference model. The diffusion coefficients do not affect the particle size ratio very dramatically.

Parameters Controlling the Nucleation Rate

The nucleation time is a parameter that is not known. Calculations (ref. 2) suggest typical times for heterogeneous nucleation are very short and we have arbitrarily chosen to use 10^6 sec in our reference model. Longer times would contradict the theoretical calculations and would also be comparable to other physical time constants (fig. 2). Nucleation is not a dominant process in our reference model (fig. 2) because the number of unnucleated cores is small except just above the tropopause and just below the evaporation level. Increasing the nucleation time would allow more cores to penetrate deeply into the layer and so spread the importance of nucleation over the layer. To explore the effects of different nucleation times we have performed calculations with time constants of 10^7 sec, which makes many processes faster than nucleation, and 10^5 sec. The results, shown in figures 9(a) through 9(d), demonstrate that the choice of nucleation time is not very significant. Faster nucleation has almost no effect on the results. Slower nucleation allows slightly more acid vapor to be deposited on preexisting acid particles, which increases their size slightly and decreases the size ratio.

Processes that Affect the Growth Rate

The stratospheric temperature and H_2O abundance are both variable and strongly affect the H_2SO_4 vapor pressure P_v. The growth rate is controlled by P_v when the supersaturation is low. Temperature also weakly controls the microphysical diffusion coefficients determining coagulation, growth, and sedimentation rates. Figure 10 illustrates the reference model temperature and H_2O profiles and some alternative values that have been modeled in figure 7. The reference model H_2O mixing ratio curve represents a "dry" stratosphere. Though most observers seem to favor these smaller mixing ratios in the lower stratosphere, some believe that the mixing ratio increases with altitude. The most extreme, yet still plausible, profile is that of Sissenwine et al. (ref. 32) who found that the mixing ratio increased dramatically with height. Hence, our alternative H_2O profile uses Sissenwine's values to about 30 km and assumes the mixing ratio is roughly constant at higher altitudes (where no measurements were made). Our reference model atmospheric temperature is the standard atmosphere midlatitude spring/fall profile (ref. 33). The warm and cold profiles of figure 10 are extreme values, representing July and January temperatures at latitude 75°N.

Figure 7 shows that the model is rather insensitive to increased stratospheric water vapor. The large particle and mass mixing ratios are increased slightly because the increased H_2O decreases the acid solution concentration, which in turn decreases the H_2SO_4 vapor pressure and causes the difference between the H_2SO_4 partial pressure and the H_2SO_4 vapor pressure to be larger, thereby enhancing the growth rate.

Changing the temperature strongly affects the aerosol properties (fig. 7). Below 25 km the large particle mixing ratio is more strongly modulated by temperature than is the mass mixing ratio. The mass is fixed by the sulfur gas supply, but the number of large particles is very sensitive to small changes in the size distribution which occur due to temperature-modulated supersaturation changes. Both mass and large particle mixing ratios approach zero at altitudes above the evaporation level. Of course, evaporation occurs when $S \leqslant 1$ and the level where this inequality is satisfied is controlled by P_v. The H_2SO_4 vapor pressure change for the warmer stratosphere case is so large that the vapor pressure throughout the stratosphere exceeds the reference model H_2SO_4 partial pressure by orders of magnitude. If the particle physics were not interactive with the gas phase chemistry, we would

have predicted that the entire layer had evaporated. Figure 5 shows that the chemistry readjusts the amount of acid present as vapor so that the supersaturation remains above 1 throughout most of the stratosphere in the warm stratosphere calculation. Essentially, higher temperatures reduce the condensation rate on particles of the chemically produced acid, allowing the acid level to build up until the net H_2SO_4 loss rate is about equal to that in the reference model. Cooling of the stratosphere drops the H_2SO_4 vapor pressure and increases S (fig. 5). Because the growth rate depends on the difference between partial pressure and vapor pressure, the growth rate is nearly independent of vapor pressure when P_v is small. Since the growth rate is not changed, the mass mixing ratio is little altered in the cold stratosphere calculation. The high value of S in the cold stratosphere makes homogeneous nucleation much more likely to occur than in the reference model, and homogeneous and ion nucleation should be included in a model run under these conditions.

An interesting aspect of the warm-temperature calculation is that the mean particle size increases slightly and the large particle mixing ratio decreases. This change is due to the Kelvin effect. For particles of the sizes found in our model, the Kelvin vapor pressure correction for sphericity is small and because S is normally large, the Kelvin effect is not usually of any importance in our model. However, in the high temperature case, S is so close to unity (fig. 5) (as for typical terrestrial water clouds) that the Kelvin corrections become important. Particles larger than 0.1 μm evaporate only above 30 km in the high-temperature calculation, but 0.01-μm particles evaporate everywhere except just above the tropopause. Curiously, the 0.03-μm particles evaporate and grow in several regions due to the small oscillations in S (fig. 5).

One quite interesting feature of the S curves shown in figure 5 is that their shape is not similar to the shape of the large particle mixing ratio profile, as was hypothesized by Rosen and Hofmann (ref. 34). In our model, the lower part of the layer is controlled by the tropospheric rainout sink, and the upper part is controlled by the S profile. The decreasing value of S with height is due primarily to rapidly increasing H_2SO_4 vapor pressures, resulting from increasing stratospheric temperatures at higher altitudes.

The warm- and cold-temperature calculations were done for steady-state perturbations. In reality, the temperature fluctuates with season and with stratospheric weather. The evaporation-growth process can be highly nonlinear because of the nonlinear dependence of vapor pressure on temperature. To obtain nonlinear changes, it is necessary that the partial pressure controlling growth be much less than the vapor pressure controlling evaporation. This could occur if the aerosol mass were not sufficient to supply its own vapor pressure at typical temperatures or if the acid vapor were subjected to some sink after evaporating from the particles.

To test the possible nonlinear temperature behavior, a calculation was made in which the temperature was changed every 3 months to simulate the midlatitude U.S. Standard atmospheric temperature profile changes with season (ref. 33). There is no evidence of any important nonlinearity in the model simulation since the spring and fall results were nearly identical to each other and to the reference model "steady-state" spring-fall calculations.

Two quantities in the growth equations have values that are poorly known: P_v, the H_2SO_4 vapor pressure, as determined from theoretical equations, and α, the H_2SO_4 sticking coefficient. Our model utilizes the H_2SO_4 vapor pressure expression devised by Gmitro and Vermeulen (ref. 35), which is basically a theoretical calculation of the vapor pressure. Verhoff and Banchero

(ref. 36) have shown that the expression does not agree well with room temperature P_v measurements. Even for pure H_2SO_4, the room temperature vapor pressures used by various authors differ by a factor of 100. There are no measurements of P_v at temperatures relevant for the stratosphere so the magnitude of the possible stratospheric error is not known. In figure 9, calculations were performed with the assumption that P_v is increased and decreased by a factor of 100, independent of temperature. In the reference model, P_v changes by about 10^5 between 14 and 34 km so that a factor of 100 uncertainty is much less than the total variation of P_v with altitude.

The second unknown parameter, the sticking or evaporation coefficient α, represents the probability that a molecule of H_2SO_4, colliding with an H_2SO_4 droplet in a supersaturated environment, will stick; or, conversely, the probability that, in an undersaturated environment, a molecule which might theoretically evaporate, does evaporate. Paul (ref. 37) has compiled evaporation coefficients for many substances, and although some substances have extremely small values of α, many have values lying between 0.03 and 1. A value of 0.03 seems appropriate for water (ref. 38) but there are no data for sulfuric acid. A value of 0.03 was chosen as a reasonable lower limit to use in a test and we employed a small radius-dependent correction to α suggested by Okuyama and Zung (ref. 39). For small particle sizes under stratospheric conditions, the growth rate is directly proportional to α. Thus, changing α from 1 to 0.03 is quite a significant modification of the growth equation.

Figures 9(a) through 9(d) show that changing α has very little effect on the calculated properties except that it slows evaporation slightly and so allows the particles to reach slightly greater altitudes, as shown most evidently in figure 9(d). Changing P_v affects the large particle and mass mixing ratios strongly at high altitudes by changing the evaporation level.

It is remarkable that such large changes in the growth rate due to modification of α or P_v have such small effects upon the aerosol layer. Figure 5 shows that S is strongly modified by changes in α and P_v. Reducing P_v does not alter the growth rate, except near the evaporation level, so the large increase in S is not physically significant (ignoring homogeneous and ion nucleation). However, increasing P_v or decreasing α alters S by causing a change in the partial pressure. Essentially, a reduced growth rate leads to a buildup of vapor until the net growth is nearly the same as in the reference model except, of course, above the evaporation level.

The interplay between the chemical production of H_2SO_4 vapor, H_2SO_4 storage in the vapor phase, and H_2SO_4 storage in the aerosol phase is one of the most interesting aspects of the model sensitivity studies. If the production rate changes, the vapor phase storage (and hence S) is not greatly altered because aerosol particles change their size and number to accommodate the altered rate of sulfur supply. On the other hand, if one of the characteristics of the aerosol growth equation (e.g., P_v,α,T) is changed, then the particles are relatively unchanged, but the vapor phase storage is modified. The vapor phase storage is always very small compared to the aerosol mass, except above the evaporation level. (At 16 km the vapor is 10^{-4} of the aerosol mass; at 20 it is 10^{-4}; but at 30 it is 10^{-1}.) Hence, the vapor phase H_2SO_4 storage itself is not generally an important reservoir of sulfate mass. Rather, the results suggest that the aerosol particles have relatively fixed properties for given rates of gaseous supply and a given residence time. The aerosol mass is fixed by the rate of gaseous supply. Since the number of particles is fixed by the rate of supply of nuclei (and coagulation) there is little room for a change in the aerosol properties through the modification of the growth rates.

COMPARISON WITH OBSERVATIONS

The model is applied to actual observations as each observed property of the aerosol layer is discussed in terms of our sensitivity study. Answers to the following questions were sought: What physical processes control the observed property? What future experiments related to the observed property might tell the most about aerosol physics? How might the aerosol model be improved? Why should a one-dimensional model yield agreement with observations?

Total Particle Mixing Ratio

Figures 1(a), 3(a), 4(a), 6(a), 7(a) and 9(a) present observations and sensitivity studies of the total particle number mixing ratio. It was concluded from these studies that the total particle mixing ratio is controlled almost entirely by coagulation – a process with no adjustable parameters. Junge et al. (ref. 8), Cadle and Kiang (ref. 40), and Hamill et al. (ref. 3), using simpler models, previously deduced that, by number, most stratospheric particles originate as tropospheric Cn and that the stratosphere is basically a sink for particles. The particle number is reduced by coagulation and the particle size and mass are increased by sulfate growth. Additionally, our model indicates that above 25 km the relative importance of diffusion and sedimentation partly determines whether the total particle mixing ratio declines with altitude or is nearly constant. The number of particles at the tropopause weakly controls the number of particles in the stratosphere.

Stratospheric observations of Cn are in disagreement with each other by more than an order of magnitude, but tropopause values disagree by less than a factor of 4 (fig. 1(a)). Great spatial or temporal variability in stratospheric Cn is possible, but systematic errors between these measurements are also possible. Some of the stratospheric measurements imply that different physical mechanisms are at work. For example, the early observations of Junge et al. (ref. 8) imply very slow upward mixing of the particles or a strong sedimentation sink at high altitude. On the other hand, the data of Käselau et al. (ref. 10) suggest a high-altitude particle source. Although meteoritic debris is clearly a possible source, it is also possible that the evaporation process can supply new particles. In our model, when aerosols coagulate with one another, each particle accumulates many cores. For example, in the monodispersed core calculation it was found that a typical 0.5-μm particle at 20 km contained 190 cores. However, when these particles evaporate, our model assumes that only one large core is released; in reality many cores could be released. Thus, if a particle source exists at high altitude, chemical composition studies will be needed to determine whether the source is meteoritic or evaporative.

Initially, however, further observational studies are required, preferably as a function of latitude, to define more conclusively the "normal" total particle mixing ratio in the stratosphere. Additionally, several special observations might provide important clues about stratospheric particle sources. One particle source that should be examined using total particle mixing ratio data as a basis is direct particle injection due to rocket and aircraft flights and volcanic explosions. Calculations of the stratospheric aerosol properties, especially particle size, following a volcanic explosion depend critically on whether ash particles are injected and on whether homogeneous or ion nucleation occurs. If all the sulfur gases emitted by the volcano are deposited on preexisting stratospheric particles, then the particles will be larger than if the sulfur gases are also deposited on cores

provided by the volcanic eruption. Climate calculations (e.g., ref. 41) are quite sensitive to particle size and even the sign of the climate change can be altered if the size is not correctly known.

Rosen and Hofmann (ref. 11) reported an increase in the number of large particles following the Fuego eruption, but no change in the total number of particles, suggesting that H_2SO_4 was deposited directly onto preexisting particles. It is important to examine other eruptions as well. For proper modeling to be accomplished, simultaneous measurements of the total number of particles, the number of large particles, the amount of volcanic ash, and the number of particles not containing cores (obtained by heating the intake air to the condensation counter) are needed before and after the eruption. It should be noted that only one large eruption – Agung in 1963 – has occurred during the last 65 years and theoretical studies of aerosol formation and radiative transfer-climate effects following that eruption have been hampered by a lack of information about the resultant ratio of sulfate to silicate ash. Filter samples taken during and after the Agung eruption have been successfully analyzed for sulfate (ref. 20) and filters are apparently still available to any interested experimentalist for analysis of Si, or any other element diagnostic of silicate ash.

Particles may also be injected directly into the stratosphere by space shuttle and aircraft engines. Brownlee et al. (ref. 18) have found small numbers of Al_2O_3 spheres from rocket exhaust in the stratosphere. Rosen and Hofmann (ref. 34) have suggested that future space shuttle flights might greatly increase the ambient number of small particles at high altitudes. Rosen et al. (ref. 13) measured large numbers of Cn just below the tropopause and argued that these particles were produced by jet aircraft. If large numbers of aircraft enter the stratosphere and deposit Cn it could be significant for the total particle count. Hence, further *in situ* measurements of the particulates associated with aircraft emissions and with possible future rocket ejecta are important to make. Theoretical studies of the effects of the particulate emissions on the stratospheric aerosol layer are now being conducted (refs. 1, 34).

The final important source of total particles requiring observational study is homogeneous-heteromolecular and ion nucleation. Such nucleation may be significant after volcanic explosions or when the stratosphere is cold. Figure 5 shows that the supersaturation ratio is large over a large portion of the stratosphere when temperatures are low. Homogeneous nucleation is difficult to detect under normal stratospheric conditions, if it occurs at all, because the nucleation rates needed to produce the observed number of stratospheric particles are low, and because any pure acid-water particles will quickly coagulate with preexisting particles, some of which contain cores. One technique for detecting homogeneous nucleation would be to examine a cooling air mass in which the total number of Cn should continuously and rapidly increase if homogeneous nucleation is significant.

It is curious to note that the only observed stratospheric clouds, mother of pearl clouds, occur near 25 km during late winter months in both hemispheres when temperatures fall below $-80°C$, the lowest values found in the stratosphere. Cooling temperatures seem to precede cloud formation (refs. 42-45). Hallett and Lewis (ref. 42) previously suggested that the clouds might contain H_2SO_4. In addition, Hesstvedt (quoted in ref. 44) has shown that homogeneous nucleation of water will not occur for typical stratospheric water vapor amounts, so that stratospheric sulfuric acid particles are needed as nuclei. The acid particles will not serve as water droplet nucleation centers but, as the water vapor pressure increases, will grow continuously at effective H_2O supersaturations far below 1 with respect to those for pure water. It is also possible that homogeneous heteromolecular or ion nucleation will occur, leading to large numbers of new small particles. Therefore, observation of a

stratospheric cloud does not necessarily mean that the stratosphere is saturated with respect to water as assumed by Stanford (refs. 44, 45). Better theoretical (and especially observational) studies of mother of pearl clouds would reveal information useful in studying nucleation and stratospheric water vapor amounts. Of course, if the mass of mother of pearl clouds is comparable to the mass of H_2O in the stratosphere, then H_2SO_4 cannot be significant in the cloud after formation because the mass of H_2SO_4 is a very small fraction (10^{-3}) of the H_2O mass in the stratosphere.

Noctilucent clouds occur at the summer mesopause (~80 km) at high latitudes when temperatures reach their annual minimum values of ~140 K (refs. 43, 46). The mass mixing ratio of the noctilucent cloud particles suggested by Reid (ref. 46) is larger by 10^4 than the mixing ratio of sulfur-bearing gases above the stratospheric aerosol layer in our model. Unless there is a high altitude sulfur source, it does not seem possible for the noctilucent cloud particles to be H_2SO_4 particles. However, it is possible that the initial nucleation process of noctilucent clouds could involve heteromolecular nucleation of some type.

As pointed out, additional measurements of total particle mixing ratios are needed to define more clearly the ambient stratospheric aerosols. Therefore, it is not possible to improve our model by comparison with current data. Neither can comment be made on the utility of one-dimensional models for describing this observable.

Large Particle and Mass Mixing Ratios

Two closely related observables are the large particle and mass mixing ratios (parts (b) and (c) of figs. 1, 3, 4, 6, 7, and 9). Evaporation, sedimentation, and diffusion physically control the large particle and mass mixing ratios at high altitudes, while the mixing ratios are sensitive to the magnitude of the gaseous source of sulfur at all altitudes. At low altitudes, mixing across the tropopause and washout controls these mixing ratios. Sensitivity results (fig. 4) suggest that the observed large particle and mass mixing ratio profiles are not consistent with the assumption that all the stratospheric sulfur originates through diffusion of SO_2 across the tropopause, but rather that OCS diffusion or continual SO_2 injection above the tropopause is needed. Crutzen (ref. 47) was the first investigator to suggest the importance of OCS to the stratospheric aerosol layer. He based his ideas on the near balance between sulfur diffusing into the layer as OCS and sulfur leaving as aerosols. Our model additionally shows that the altitude profile of the large particle and mass mixing ratios and the particle size ratio are different for SO_2 and OCS sources and that observations more closely resemble calculations when an OCS source is included.

Although our model is designed to study stratospheric aerosols, our sensitivity studies do suggest that two physical mechanisms, not previously studied, might be important near the tropopause. These mechanisms are ion or homogeneous nucleation production of H_2SO_4 Cn below the tropopause and large particle production below the tropopause by falling stratospheric particles.

Homogeneous or ion nucleation of sulfuric acid, and certainly nucleation of the existing tropospheric particles, is suggested because our model yields very large supersaturations of H_2SO_4 near the tropopause and smaller values at higher and lower altitudes (fig. 5). We were not able to reduce these supersaturations by more than an order of magnitude by heterogeneously nucleating the ambient particles, although changing the H_2SO_4 vapor pressure equation did produce somewhat greater reduction. These large supersaturations occur because the temperature is low and the H_2O

concentration is large, both of which depress P_v, causing it to have a minimum near 10 km. Because the partial pressure of H_2SO_4 does not have such a minimum, S has a maximum at that altitude. Rosen and Hofmann (ref. 11) found that the total particle mixing ratio has a maximum in the upper troposphere. We are not aware of any studies showing that these Cn have an important H_2SO_4 component; however, chemical studies of upper troposphere particles are practically nonexistent.

Another interesting problem is the origin of large particles in the upper troposphere. Although these particles could have a tropospheric origin, they might also be falling stratospheric particles. The model results shown in figure 6(b) suggest that if the aerosol removal rate at 10 km is only a few days, then large particles falling from the stratosphere dominate over the large particles grown from sulfuric acid *in situ* at 10 km. Models of upper tropospheric particles, and especially experimental studies of the upper tropospheric large particles, are clearly of importance.

While our sensitivity studies have focused on the vertical profile of the large particle mixing ratio, additional insight into physical mechanisms may be gained from studies of the column integrated number of large particles. Hofmann et al. (ref. 12) have integrated their observations of the large particle mixing ratio above Laramie, Wyoming in a vertical stratospheric column to reveal an interesting linear relation between tropopause pressure and total large particle content (see fig. 11). We have performed sensitivity tests relevant to these changes by independently altering stratospheric temperatures (as in fig. 7(b), and in a seasonal calculation not shown) and tropopause height (fig. 7(b)). In our seasonal temperature calculation we found a 5% oscillation in the total number of large stratospheric aerosols over a yearly cycle. The extreme high latitude temperature changes illustrated in figure 7(b) yielded a ±30% change in the total number of particles above the tropopause. However, moving the model tropopause level up and down yielded a +100%, −50% change in the total column number of stratospheric large particles that varied nearly linearly with tropopause pressure (fig. 11). We conclude that unless stratospheric temperature changes are extreme, the normal ascent and descent of the tropopause accounts for the observations of Hofmann et al. (ref. 12). The physical processes are complex, however. For example, figure 7 and our earlier discussion showed that a lower tropopause level yields fewer total particles in the stratosphere, but more large particles. As the tropopause falls, the aerosol residence time at low altitudes increases and the supply of sulfur gas increases so that more large particles can grow. When the tropopause moves upward, aerosols at low altitudes have a shorter residence time since they are excluded from the stratosphere. It appears that residence time and gas supply are the important controlling factors rather than the supply of Cn.

Several new observations of large particles and mass need to be made. Current large particle and mass mixing ratio data above 25 km are not in agreement with each other; thus, observational evidence for evaporation, the only physical mechanism in our model that has no direct observational basis, is lacking. It is especially important to discover whether evaporation occurs since that process is sensitive to several assumptions in our model and a clear determination of the evaporation level would allow the model to be improved.

Sensitivity studies show that the location of the top of the aerosol layer in our model, which is fixed by evaporation, is strongly controlled by temperature (figs. 7(b) and 7(c)) and H_2SO_4 vapor pressure (figs. 9(b) and 9(c)). The temperature varies with time, while the H_2SO_4 vapor pressure is not well known and could be altered by dissolved impurities. It is also possible that if conditions occur in which the growth-evaporation processes are nonlinear, dynamics could be significant to the

model results. In any event, dynamically driven temperature changes clearly are important in day-to-day variability in the layer if evaporation actually occurs.

One way to investigate evaporation is to study aerosols over the poles. High temperatures occur over the summer poles, while there are deep cold regions over the winter poles. Thus, if evaporation is a significant physical mechanism, the aerosol layer may extend to higher altitudes over the winter poles than over the summer poles. Satellite observations may be ideal for detecting such variations. Current balloon measurements do not show any obvious difference between aerosols over winter and summer poles, but winter observations may not extend far enough poleward to reach the area of high altitude cold air. Rosen et al. (ref. 13) have shown that the winter (Feb.-Mar. 1973) maximum polar large particle mixing ratio occurs about 7 km higher than does the maximum fall mixing ratio (Nov. 1973).

A second way to study evaporation is to obtain new data above 25 km. The large particle mixing ratio results of figure 1(b) hint that the layer has a peak mixing ratio around 20 km and a declining mixing ratio above, suggesting that evaporation occurs near 25 km. However, the observations do not extend to high enough altitudes to confirm the decline. The mass mixing ratio profile (fig. 1(c)), on the other hand, does not show a decline in mass mixing ratio at 25 km. Lazrus and Gandrud (refs. 15, 48) believe the mass mixing ratio of sulfate is constant up to 37 km, implying that evaporation occurs above 37 km or does not occur at all. If future large particle data show a decline at 25 km, while mass mixing ratio data do not, the two data sets will clearly be in disagreement. It should be noted, however, that the aerosol layer evaporates at a level where the mass mixing ratio of the aerosol is comparable to that in the vapor phase (compare fig. 1(c) of this paper and fig. 5 of ref. 1). It is known that the filters used to make the mass mixing ratio measurements collect some gases, and they will apparently collect H_2SO_4 vapor as well (Lazrus, private communication, 1977). Thus, the high altitude mass mixing ratio data may not indicate that aerosols reach such high altitudes, but rather that H_2SO_4 vapor does.

Several existing data sets are relevant to the question of evaporation at high altitudes. Bigg et al. (refs. 49, 50) made impactor collections at altitudes as high as 40 km. They identified (morphologically) the particles between 15 and 25 km as sulfuric acid droplets, but above 30 km Bigg et al. found no particles containing H_2SO_4. These observations agree with our model results. Bigg et al. (ref. 49) also presented a particle concentration mixing ratio curve which, neglecting collection efficiency problems, was independent of height from 25 to 35 km. This is also consistent with our model. Figure 1(a) shows that the total particle mixing ratio is almost constant with altitude in the 25 to 35 km region. As sulfuric acid evaporates in our model, a nonvolatile core is left behind whose concentration mixing ratio can be independent (or even increasing) with height if more than one core is released by each evaporated particle. Our model also suggests that the mean particle size should decrease with altitude, especially if the particle cores are a negligible fraction of the total particle volume. However, no clear size change with altitude is noted in the work of Bigg et al. (refs. 49, 50).

A second relevant data set has been obtained by lidar studies of the aerosols. Lidars measure the backscattering from stratosphere aerosols and are sensitive mainly to larger ($r > 0.1$ μm) particles. An absolute measurement of particle concentration is not obtained. However, the ratio of the total scattering (aerosols plus gases) to gas scattering often shows a value of unity at altitudes below the stratospheric aerosol layer, but an ill-defined broad aerosol layer with nonunit scattering ratio may extend to 35 km (ref. 51). This broad layer may indicate that the aerosols do not

evaporate until close to, or above, 35 km (as in our reference model), or that the H_2SO_4 particles contain large cores that continue to influence the lidar results after the acid evaporates.

Hofmann and Rosen (ref. 52) presented measurements of large particle concentration at ambient temperatures and large particle concentration with the air heated to 150°C. Presumably, heating the air will quickly lead to sulfuric acid evaporation. The important result is that near 28 km (where the measurements stopped), the two results were almost identical even though they strongly disagreed below 28 km. This could indicate that the heated air sample was at the lower particle sampling limit of the instrument so that convergence of the two measured concentrations is meaningless. However, it may also indicate that the aerosols normally evaporate near 30 km so that heating of the aerosols near 30 km leads to no further reduction in the number of large particles. Evidently, more measurements at high altitude and greater sensitivity are needed.

At present our model assumes that the cores are inert, that the cores do not grow in the stratosphere, and that the cores are not the dominant aerosol in the stratosphere. These assumptions require careful experimental verification; further experimental information about core composition and origin would allow our model to be improved. One technique for learning more about the cores is to make measurements of the particulate mass mixing ratio altitude profiles of chemicals other than sulfates. Of particular interest would be those of NH_3, Si, Fe, C, Cℓ, Na, and H_2O. According to our model, particulate H_2O and relative humidity independently determine the aerosol H_2SO_4 concentration so that by measuring both quantities a cross check on vapor pressures can be made. Si, C, Cℓ, Na, and Fe mixing ratio profiles might determine whether meteorite debris is significant for the layer, or if any of these elements come from the troposphere. Substantial quantities of C would be optically significant. It has long been suggested that NH_3 might reach the stratosphere as a gas and form particulates; if so, its particulate mixing ratio should increase with height in the stratosphere.

Our one-dimensional model predictions of mass and large particle mixing ratios are in good agreement with observations except above 25 km, where the observations are poor. Data show that the mass and large particle mixing ratios are roughly identical in both hemispheres and that isopleths dip downward from the equator toward the pole. The peak large particle mixing ratio is about 50% larger over the equator than the pole.

We believe that there are two reasons for these observations and for the success of a one-dimensional model in predicting local mass and large particle mixing ratios. First, the aerosol layer is apparently trapped between the tropopause, below which there is rapid removal due to rainout, and the evaporation level, above which the aerosols are quickly depleted by vaporization. Neither the tropopause height, nor the stratospheric temperature has strong latitudinal variation (although there is some variation). Thus, the aerosol layer is not free to display much different structure than is observed, and a one-dimensional model with a realistic local tropopause height and temperature profile will be successful in roughly locating the layer. The second reason the one-dimensional model is successful and the aerosols are relatively uniformly distributed globally is that OCS has a very long lifetime and is thus nearly uniformly distributed. Thus, as particles move about in the stratosphere they are subjected to nearly constant supplies of sulfur-bearing gases; consequently the particles grow to roughly similar sizes at all locations. Of course, horizontal transport is quite fast compared with aerosol residence time of ~2 years at 20 km which also helps keep the aerosols well mixed.

The principal observations that require use of a two-dimensional simulation are the latitudinal slope of the mixing ratio isopleths and the mixing ratio peak, which has a 50% larger magnitude at the equator than at the poles (e.g., ref. 13). Although plausible, it is not certain that a greater magnitude of the mixing ratio at the equator signifies an equatorial source of sulfur as suggested by Rosen et al. (ref. 13). Figures 7(b) and 7(c) show that low temperatures and a lower tropopause in a one-dimensional model both signify a higher mass mixing ratio than higher temperatures and a high tropopause. Since the equator is characterized by a high tropopause and low temperatures compared with polar regions, there are competing effects. Also, OCS decomposition to form H_2SO_4 requires ultraviolet sunlight, whose intensity is a function of latitude. Therefore, a two-dimensional aerosol model is required to separate the effects of transport from those of aerosol physics and chemistry in the latitudinal gradient of particle mixing ratio.

Size Distribution

The final observables are the size distribution and the related particle size ratio. The particle size ratio (0.15 to 0.25 μm radius) is strongly controlled by growth and sedimentation (fig. 3(d)). By comparison, the small particle end of the size distribution is controlled by coagulation, while the largest particles are sensitive to the number of large cores that are available and to water vapor growth. Altering the source strength (fig. 4(d)), tropopause height, or stratospheric temperature (fig. 7(d)) can change the size ratio by a large factor. In reference 1 we developed a simple analytic model for a growing aerosol in which the size distribution depends only on the initial particle size and the product of residence time and growth rate. Our sensitivity studies show this same dependence, with the initial particle size being determined in some approximate sense by coagulation and to a lesser extent by the core size distribution.

Observations of the aerosol size distribution are sparse. Figure 1(e) indicates that the reference model size distribution is in good agreement with the average of the available measurements. The available size measurements do not adequately portray the size distribution below 0.1 μm, however, and our model results show a strong altitude dependence for small particle sizes, as do integrated measurements (compare figs. 1(a) and 1(b)). Observed concentrations of very large particles (>1 μm) may be slightly greater than those predicted by our reference model, although there are very few observations on which to base a comparison. Brownlee et al. (ref. 18) presented data showing that rocket exhaust particles dominate the size range 3 to 8 μm and meteoretic debris dominates larger sizes. We have found that even with a very steep tropospheric Cn size distribution in our model, the particles near 1 μm are mostly composed of cores. Thus, the large particle end of the distribution is probably not controlled by H_2SO_4 growth, but is determined in model simulations by assumptions about the supply of inert large particles.

In our reference model, particles residing in different size ranges originate from distinctly different sources. The smallest and largest particles are essentially "wet" core particles, while intermediate size particles are mainly H_2SO_4–H_2O solution droplets. Whitby and his coworkers (e.g., ref. 53) have shown that tropospheric aerosols also have many sources and that surface and volume concentration plots often have a multimodal structure revealing these sources. Consequently, in figure 12, we have replotted our size distributions in terms of particle surface and volume concentration. Of greatest interest in figure 12 are the curves for 16 km, which are clearly bimodal. The two peaks occur because large particles tend to form at higher altitudes, where the residence time is long, while small particles originate near the tropopause, where small cores are

available. Friend (ref. 54) presented a conceptual model of the aerosol size distribution having one peak near 0.3 μm and another well below 0.1 μm. Current experimental studies (e.g., ref. 17) do not favor such a distribution in an average sense. However, it is quite reasonable that individual collections of stratospheric particles should yield bimodal distributions. The bimodal structure in figure 12 is due to the mixing of two separate distributions. In the atmosphere, mixing processes are much more random than can be simulated by a one-dimensional model, so the degree of bimodality ought to be more pronounced in nature than in our model simulation.

Note in figure 12 that the mass mean radius is $\sim$2 μm. There have been suggestions (e.g., ref. 55) based on indirect optical techniques, that most aerosol mass must be in the size range below 0.1 μm and that the numbers of small particles must greatly exceed those measured by Cn counters (fig. 1(a)). Our model results suggest that observed Cn counts are quite consistent with observed mass concentrations and size distributions and that the occurrence of large unmeasured concentrations of small particles is unlikely.

Our model results suggest the value of making a number of future observations of aerosol size distributions. Current particle size ratio data show a weak dependence on altitude which is crudely matched by our model. Near the tropopause, smaller particles are found (fig. 1(d)), since little H_2SO_4 growth has occurred, but our model has slightly too many small particles near the tropopause. This could be corrected by using a Dickinson-Chang-like diffusion profile, by modifying the Cn size profile near the tropopause, by increasing the rainout time, or by allowing homogeneous or ion nucleation below the tropopause. It would be particularly interesting to measure the upper tropospheric aerosol size distribution in order to partly determine which of these modifications is the correct one.

Measurements of the particle size ratio above 25 km may be useful for determining the diffusion coefficient as well as the evaporation level. The reference model size ratio shows a distinct increase at the evaporation level (fig. 1(d)). Figure 7(d) demonstrates that use of a smaller eddy diffusion coefficient (Hunten's) at high altitudes leads to a gentle bend in the ratio near 25 km.

Present size distribution data do not show any obvious latitudinal trends. This behavior may be due to horizontal mixing, which is rapid compared to growth and residence times, and to nearly uniform distribution of OCS. Of course, a one-dimensional model can easily fit data with no latitude dependence. However, it is widely believed that gaseous and particulate materials (OCS, Cn) actually enter the stratosphere in the tropics (e.g., ref. 56). If so, the equatorial particles ought to be smaller than the high latitude particles. New size data should be examined for such a trend.

Current size distribution measurements do not extend below 0.1 μm. Most particles in the stratosphere (by number) are smaller than 0.1 μm and size measurements should be made in this size range. Such measurements might be valuable for identifying particle sources. For instance, homogeneous or ion nucleation might create strongly bimodal distributions below 0.1 μm.

Two properties of the stratospheric aerosol that have not been previously measured are the core volume fraction of the sulfuric acid droplets as a function of size and the size distribution of unnucleated particles. These are shown for the reference model in figures 13 and 14.

The core volume fraction is large for small particles because the particles form on cores, forcing the smallest particles (0.01 μm) in our model to be 100% core. Particles of size near 0.1 μm

are primarily produced by H_2SO_4 growth and so have small core volume fractions. However, large particles tend to have big core volume fractions.

At 16 km the largest particles are mainly damp cores. At higher altitudes the H_2SO_4 growth rate is faster and the residence time is greater so that some large particles can be produced by growth. In addition, the very large Cn fall so rapidly that they do not mix efficiently to high altitudes. However, at some sizes substantial quantities of core particles still reach higher altitudes, thus leading to high core volume fractions. The effect diminishes with increasing altitude. The precise nature of the core volume fraction increase with size depends upon the assumed core size distribution. For example, our r^{-3} Cn size distribution calculations (fig. 7) have a minimum in the core volume fraction at 20 km near 0.3 μm while the minimum is near 0.5 μm for the reference model r^{-4} Cn size distribution. If cores actually grow within the H_2SO_4 droplets, further changes can occur; indeed, Hamill et al. (ref. 3) have suggested that such changes in core volume fraction might be diagnostic of core growth.

The core volume fraction is sensitive to complex interactions, such as homogeneous nucleation, Cn size, and core growth. Experiments designed to detect core volume fraction might provide insight into these mechanisms. For example, if homogeneous or ion nucleation does not occur, then small particles must be composed mainly of core material, but if such nucleation does occur, small particles can be largely acid. Although it would be of interest to have good observations of core volume fraction, such measurements may be difficult. Bigg (refs. 7, 57) presented two observations, illustrated in figure 13. Unfortunately, these data (taken in the same location at the same time with the same technique) do not agree with each other or with our model predictions.

Another variable related to the core volume fraction is the square root of the core volume second moment (fig. 13). The standard deviation of the core volume in an acid droplet of a given size is the difference between the squares of these two quantities. Growth and coagulation lead to dispersion of the core volume. For the smallest particles, the standard deviation of the core volume is zero because the only source of these particles is the smallest size Cn in our model. The standard deviation increases with radius because moderate size particles originate (by growth and coagulation) from Cn and acid particles of widely separated sizes. Very large particles have lower standard deviations because they have not grown or coagulated appreciably from the original Cn radius.

Figure 14 presents the size distribution of the unnucleated particles. At 16 km, the base of the aerosol layer, there are only 1% as many Cn as at the tropopause, but the Cn constitute about 10% of the total number of particles. The large particles are preferentially depleted from the unnucleated core distribution by coagulation because small acid particles rapidly collide with the large Cn, converting them into acid particles. If nucleation were more rapid than coagulation, the effect would be unimportant, so this is a model-dependent phenomenon. At 36 km, above the evaporation level, all the particles are bare cores and their number is about 0.1% the number at the tropopause; the small core particles have been lost due to droplet coagulation. At 30 km, about 10% of all the particles are unnucleated cores that have come from above the evaporation level, as is clear from the similarity of the size distribution at 30 and 36 km. At 20 km, however, the Cn have a size distribution similar to that in the troposphere, since 20 km is closer to the troposphere (12 km) than to the evaporation level (34 km) and the troposphere is a stronger Cn source. At 20 km, only 0.5% of the total number of particles are Cn in the reference model.

CONCLUSIONS

In the preceding sections, we have examined the sensitivity of our aerosol model to the physical processes and adjustable parameters contained in the model. We classify the sensitivity as: high, if the differences between calculations of a quantity are greater than the natural variability of the observed quantity; moderate, if the differences are of the same magnitude as the natural variability; and low, if the differences are much less than the natural variability. Here, natural variability is meant to include experimental errors accompanying the observations. The results of the sensitivity analyses are summarized in table 1.

Comparison of the model with observational data and consideration of the sensitivity studies in table 1 lead to a number of conclusions concerning the basic physical and chemical processes governing the stratospheric aerosol layer. The total particle mixing ratio is controlled mainly by coagulation, but the number of Cn at the tropopause and the diffusion coefficient at high altitudes are also important. The mass and large particle mixing ratios are controlled by growth, sedimentation, and particle removal by both evaporation at high altitudes and by washout below the tropopause. The sulfur gas source strength and the aerosol residence time in the stratosphere are much more important than the supply of Cn in establishing mass and large particle concentrations. Although the particle size in the range between 0.1 μm and 1 μm is also controlled by residence time and sulfur gas source strength, coagulation dominates at very small sizes and the Cn concentration dominates at very large sizes. Observed concentrations of tropospheric OCS and SO_2 appear sufficient to create the observed unperturbed aerosol layer characteristics, if we consider only their transport across the tropopause. OCS dominates the unperturbed layer in our model, but SO_2 could be important if it were directly injected into the stratosphere. The latter gas does strongly influence the number of particles just above the tropopause where particle concentrations, rather than mixing ratios, are highest.

We believe that our present reference model is in good agreement with the available observations and is not strongly biased by any uncertain parameters. However, the model can certainly be improved and further observations would be helpful in this regard. The most important prospective model improvements are: development of a two-dimensional model so that latitudinal variations can be studied; development of a scheme to allow the acid droplets to interact with their cores and with additional stratospheric gases so that the chemistry and H_2SO_4 vapor pressure of aerosols can be better represented; improvement of the H_2SO_4–H_2O vapor pressure equation so that the evaporation level and supersaturation can be more precisely predicted; and development of homogeneous-heteromolecular and ion nucleation schemes to determine whether such nucleation is significant under abnormal stratospheric conditions.

A number of new observations are needed. Measurements of total particle mixing ratios are needed to define the ambient aerosol properties and to search for evidence of high altitude or *in situ* particle formation mechanisms. Aerosol observations in a cooling air mass might be of particular interest for detecting homogeneous and ion nucleation. Observations of the mass and large particle mixing ratio at altitudes above 25 km would be useful to determine whether the H_2SO_4 particles actually evaporate there. Measurements of large particle concentrations over the cold winter and the hot summer poles, perhaps from satellites, may also reveal whether evaporation plays a significant role in the aerosol distribution. Analyses of particulate mass mixing ratio profiles of trace constituents such as NH_3, Si, Fe, Na, C, Cℓ, and H_2O might reveal information about the sources of

aerosol cores, the growth from the gas phase of these cores, and the sulfuric acid concentration. The aerosol size distribution needs to be measured more extensively to search for latitudinal trends. In addition, the size distribution of small particles should be determined as a check for homogeneous nucleation. It would also be of considerable interest to determine the core volume fraction as a function of size in order to detect homogeneous nucleation and core growth.

Observations are needed near the tropopause to determine the Cn size and composition there. After a volcanic eruption it will be necessary to monitor the ratio of acid to volcanic ash, the number of large particles, the total number of particles, and the number of particles without cores in order to make good perturbation models of such events. The ratio of acid to silicate ash after the Agung eruption of 1963 can probably still be determined from existing filter collections and should be done. Observations of sulfur gases emitted from anthropogenic pollution sources (e.g., high-flying aircraft and tropospheric gaseous sulfur sources) are important to ensure that the aerosol layer is not inadvertently modified by anthropogenic means. In addition, the anthropogenic supply of Cn to the upper atmosphere needs to be monitored.

It is believed that the aerosol model discussed here will be of great value for studies of aerosol properties during perturbed stratospheric conditions and for studies of natural variations in the ambient stratospheric aerosols. The model is highly sensitive to a number of variables. The limitations placed on the model by available computer capacity and present physical and chemical knowledge are as small as currently possible. The aerosol properties calculated with the reference model appear to be in good agreement with observations.

Ames Research Center
National Aeronautics and Space Administration
Moffett Field, California 94035, September 8, 1978

REFERENCES

1. Turco, R. P.; Hamill, P.; Toon, O. B.; Whitten, R. C.; and Kiang, C. S.: The NASA-Ames Research Center Stratospheric Aerosol Model. I. Physical Processes and Numerical Analogs. NASA TP-1362, 1979.

2. Hamill, Patrick; Kiang, C. S.; and Cadle, R. D.: The Nucleation of H_2SO_4 Solution Aerosol Particles in the Stratosphere. J. Atmos. Sci., vol. 34, no. 1, 1977, pp. 150-162.

3. Hamill, Patrick; Toon, O. B.; and Kiang, C. S.: Microphysical Processes Affecting the Stratospheric Aerosol Particles. J. Atmos. Sci., vol. 34, no. 7, 1977, pp. 1104-1119.

4. Farlow, N. H.; Snetsinger, K. G.; Lem, H. Y.; Hayes, D. M.; and Trooper, B. M.: Nitrosyl Sulfuric Acid in Stratospheric Aerosols. Trans. AGU (EOS), vol. 58, no. 12, 1977, p. 1148.

5. Snetsinger, K. G.; Farlow, N. H.; Lem, H. Y.; and Hayes, D. M.: Composition and Origin of Granules in Stratospheric Aerosols. Trans. AGU (EOS), vol. 58, no. 12, 1977, pp. 1148.

6. Farlow, Neil H.; Hayes, Dennis M.; and Lem, Homer Y.: Stratospheric Aerosols: Undissolved Granules and Physical State. J. Geophys. Res., vol. 82, no. 31, 1977, pp. 4921-4929.

7. Bigg, E. K.: Stratospheric Particles. J. Atmos. Sci., vol. 32, no. 5, 1975, pp. 910-917.

8. Junge, Christian E.; Chagnon, Charles W.; and Manson, James E.: Stratospheric Aerosols. J. Meteor., vol. 18, no. 1, 1961, pp. 81-108.

9. Podzimek, J.; Haberl, J. B.; and Sedlacek, W. A.: Recent Measurements of Aitken Nuclei in the Lower Stratosphere. Proceedings of the Fourth Conference on the Climatic Impact Assessment Program, 1975. T. M. Hard and A. J. Broderick, eds., National Technical Information Service, Springfield, Va., 1976, pp. 519-526.

10. Käselau, K. H.; Fabian, P.; and Rohrs, H.: Measurements of Aerosol Concentration up to a Height of 27 km. Pure and Applied Geophysics, vol. 112, no. 6, 1974, pp. 877-885.

11. Rosen, J. M.; and Hofmann, D. J.: Balloon-Borne Measurements of Condensation Nuclei. J. Appl. Meteor., vol. 16, no. 1, 1977, pp. 56-62.

12. Hofmann, D. J.; Rosen, J. M.; Pepin, T. J.; and Pinnick, R. G.: Stratospheric Aerosol Measurements. I: Time Variations at Northern Midlatitudes. J. Atmos. Sci., vol. 32, no. 7, 1975, pp. 1446-1456.

13. Rosen, J. M.; Hofmann, D. J.; and Laby, Jean: Stratospheric Aerosol Measurements. II: The World-Wide Distribution. J. Atmos. Sci., vol. 32, no. 7, 1975, pp. 1457-1462.

14. Cadle, R. D.; and Langer, Gerhard: Stratospheric Aitken Particles Near the Tropopause. Geophys. Res. Lett., vol. 2, no. 8, 1975, pp. 329-332.

15. Lazrus, A. L.; and Gandrud, B. W.: Stratospheric Sulfate Aerosol. J. Geophys. Res., vol. 79, no. 4, 1974, pp. 3424-3431.

16. Pinnick, R. G.; Rosen, J. M.; and Hofmann, D. J.: Stratospheric Aerosol Measurements. III: Optical Model Calculations. J. Atmos. Sci., vol. 33, no. 2, 1976, pp. 304-314.

17. Toon, Owen B.; and Pollack, James B.: A Global Average Model of Atmospheric Aerosols for Radiative Transfer Calculations. J. Appl. Meteor., vol. 15, no. 3, 1976, pp. 225-246.

18. Brownlee, D. E.; Ferry, G. V.; and Tomandl, D.: Stratospheric Aluminum Oxide. Science, vol. 191, no. 4232, 1976, pp. 1270-1271.

19. Martell, E. A.: The Size Distribution and Interaction of Radioactive and Natural Aerosols in the Stratosphere. Tellus, vol. 28, no. 5, 1966, pp. 486-498.

20. Castleman, A. W., Jr.; Munkelwitz, H. R.; and Manowitz, B.: Isotopic Studies of the Sulfur Component of the Stratospheric Aerosol Layer. Tellus, vol. 26, no. 1-2, 1976, pp. 222-234.

21. Hofmann, D. J.; Rosen, J. M.; and Pepin, T. J.: Global Measurements of the Time Variations and Morphology of the Stratospheric Aerosol. Conference on the Climatic Impact Assessment Program, 3rd, Cambridge, Mass., 1974, Proceedings, Anthony J. Broderick and Thomas M. Hard, eds. (AD/A-003 846/3ST). NTIS, Springfield, Va., 1974, pp. 284-297.

22. Hanst, Philip L.; Spiller, Lester L.; Watts, D. M.; Spencer, John W.; and Miller, Matthew F.: Infrared Measurements of Fluorocarbons, Carbon Tetrachloride, Carbonyl Sulfide, and Other Atmospheric Trace Gases. J. Air Pollut. Contr. Ass., vol. 25, no. 12, 1975, pp. 1220-1226.

23. Sandalls, F. J.; and Penkett, S. A.: Measurements of Carbonyl Sulfide and Carbon Disulphide in the Atmosphere. Atmos. Environ., vol. 11, no. 2, 1977, pp. 197-199.

24. Jaeschke, W.; Schmitt, R.; and Georgii, H.-W.: Preliminary Results of Stratospheric SO_2 Measurements. Geophys. Res. Lett., vol. 3, no. 9, 1976, pp. 517-519.

25. Martell, E. A.; and Moore, H. E.: Tropospheric Aerosol Residence Times: A Critical Review. J. De Rech. Atmos., vol. 8, no. 3-4, 1974, pp. 903-910.

26. Moore, H. E.; Poet, S. E.; and Martell, E. A.: ^{222}Rn, ^{210}Pb, ^{210}Bi, and ^{210}Po Profiles and Aerosol Residence Times Versus Altitude. J. Geophys. Res., vol. 78, no. 30, 1973, pp. 7065-7075.

27. Charlson, R. J.; Vanderpol, A. H.; Covert, D. S.; Waggoner, A. P.; and Ahlquist, N. C.: Sulfuric Acid-Ammonium Sulfate Aerosol: Optical Detection in the St. Louis Region. Science, vol. 184, no. 4133, 1974, pp. 156-158.

28. Cunningham, P. T.; and Johnson, S. A.: Spectroscopic Observation of Acid Sulfate in Atmospheric Particulate Samples. Science, vol. 191, no. 4222, 1976, pp. 77-79.

29. Wofsy, Steven C.; and McElroy, Michael B.: On Vertical Mixing in the Upper Stratosphere and Lower Mesosphere. J. Geophys. Res., vol. 78, no. 15, 1973, pp. 2619-2624.

30. Johnston, Harold S.; Kattenhorn, David; and Whitten, Gary: Use of Excess Carbon 14 Data to Calibrate Models of Stratospheric Ozone Depletion by Supersonic Transport. J. Geophys. Res., vol. 81, no. 3, 1976, pp. 368-380.

31. National Academy of Sciences, National Research Council. Panel on Atmospheric Chemistry, Halocarbons, Effects on Stratospheric Ozone. Nat. Acad. Sci., Washington, D.C., 1976, p. 106.

32. Sissenwine, N.; Grantham, D. D.; and Salmela, H. A.: Mid-Latitude Humidity to 32 km. J. Atmos. Sci., vol. 25, no. 6, 1968, pp. 1129-1140.

33. COESA, U.S. Standard Atmosphere Supplements, 1966. Gov. Printing Office, Wash., D.C., 1967.

34. Rosen, J. M.; Hofmann, D. J.; and Singh, S. P.: A Steady State Stratospheric Aerosol Model. J. Atmos. Sci., vol. 35, 1978, pp. 1304-1313.

35. Gmitro, John I.; and Vermuelen, Theodore: Vapor-Liquid Equilibria for Aqueous Sulfuric, Acid, AIChEJ., vol. 10, no. 5, 1964, pp. 740-746.

36. Verhoff, F. H., and Banchero, J. T.: A Note on the Equilibrium Partial Pressures of Vapors Above Sulfuric Acid Solutions. AIChE J., vol. 18, no. 6, 1972, pp. 1265-1268.

37. Paul, B.: Compilation of Evaporation Coefficients. ARS J., vol. 32, no. 9, 1962, pp. 1321-1328.

38. Chodes, N.; Warner, J.; and Gagin, A.: A Determination of the Condensation Coefficient of Water From the Growth Rate of Small Cloud Droplets. J. Atmos. Sci., vol. 31, no. 5, 1974, pp. 1351-1357.

39. Okuyama, Masataka; and Zung, Joseph T.: Evaporation-Condensation Coefficient for Small Droplets. J. Chem. Phys., vol. 46, no. 5, 1967, pp. 1580-1585.

40. Cadle, R. D.; and Kiang, C. S.: Stratospheric Aitken Particles. Rev: Geophys. Space Phys., vol. 15, no. 2, 1977, pp. 195-202.

41. Pollack, James B.; Toon, Owen B.; Sagan, Carl; Summers, Audrey; Baldwin, Betty; and Van Camp, Warren: Volcanic Explosions and Climatic Change: A Theoretical Assessment. J. Geophys. Res., vol. 81, no. 6, 1976, pp. 1071-1083.

42. Hallett, J.; and Lewis, R. E. J.: Mother of Pearl Clouds. Weather, vol. 22, no. 2, 1967, pp. 56-65.

43. Stanford, John L.; and Davis, John S.: A Century of Stratospheric Cloud Reports: 1870-1972. Bull. Amer. Meteor. Soc., vol. 55, no. 3, 1974, pp. 213-219.

44. Stanford, John L.: Possible Sink for Stratospheric Water Vapor at the Winter Antarctic Pole. J. Atmos. Sci., vol. 30, no. 7, 1973, pp. 1431-1436.

45. Stanford, John L.: Stratospheric Water-Vapor Upper Limits Inferred From Upper-Air Observations: Part 1, Northern Hemisphere. Bull. Amer. Meteor. Soc., vol. 55, no. 3, 1974, pp. 194-212.

46. Reid, George C.: Ice Clouds at the Summer Polar Mesopause. J. Atmos. Sci., vol. 32, no. 3, 1975, pp. 523-535.

47. Crutzen, Paul J.: The Possible Importance of CSO for the Sulfate Layer of the Stratosphere. Geophys. Res. Lett., vol. 3, no. 2, 1976, pp. 73-76.

48. Lazrus, A. L.; and Gandrud, B. W.: Stratospheric Sulfate at High Altitudes. Geophys. Res. Lett., vol. 4, no. 11, 1977, pp. 521-522.

49. Bigg, E. K.; Ono, A.; and Thompson, W. J.: Aerosols at Altitudes Between 20 and 37 km. Tellus, vol. 22, no. 5, 1970, pp. 550-563.

50. Bigg, E. K.; Kviz, Z.; and Thompson, W. J.: Electron Microscope Photographs of Extraterrestrial Particles. Tellus, vol. 23, no. 3, 1971, pp. 247-260.

51. Russell, Philip B.; and Hake, Richard D., Jr.: The Post-Fuego Stratospheric Aerosol: Lidar Measurements, With Radiative and Thermal Implications. J. Atmos. Sci., vol. 34, no. 1, 1977, pp. 163-177.

52. Hofmann, D. J.; and Rosen, J. M.: Balloon Observations of the Time Development of the Stratospheric Aerosol Event of 1974-1975. J. Geophys. Res., vol. 82, no. 9, 1977, pp. 1435-1440.

53. Willeke, K.; and Whitby, K. T.: Atmospheric Aerosols: Size Distribution Interpretation. Air Pollut. Contr. Ass. J., vol. 25, no. 5, 1975, pp. 529-534.

54. Friend, James P.: Properties of the Stratospheric Aerosol. Tellus, vol. 18, no. 2-3, 1966, pp. 465-473.

55. Hirono, M.; Fujiwara, M.; and Itabe, T.: Behavior of the Stratospheric Aerosols Inferred From Laser Radar and Small Ion Radiosonde Observations. J. Geophys. Res., vol. 81, no. 9, 1976, pp. 1593-1600.

56. Reiter, Elmar R.: Stratospheric-Tropospheric Exchange Processes. Rev. Geophys. Space Phys., vol. 13, no. 4, 1975, pp. 459-474.

57. Bigg, E. K.; and Ono, A.: Size Distribution and Nature of the Stratospheric Aerosols. Proc. Inter. Conf. Structure, Composition and General Circulation of the Upper and Lower Atmospheres and Possible Anthropogenic Perturbations, University of Melbourne, Jan. 14-25, 1974, pp. 144-157. (Available from IAMAP, Atmospheric Environment Service, Downsview, Ontario, Canada.)

TABLE 1.– MODEL SENSITIVITY

Variable	Total particle mixing ratio[a]	Large particle mixing ratio[a]	Sulfate mass mixing ratio[a]	Particle size ratio[a]
I. Sinks and sources of gases:				
a. OCS, SO_2 tropospheric concentration varies	L	H	H	H
b. SO_2 injection occurs	L	H	H	M
c. HSO_3 condenses	L	L	L	L
d. OH concentration varies	L	L	L	L
II. Particle residence time, core supply:				
a. Tropopause height changes	M	H	H	H
b. Diffusion coefficient changes	M	M	M	L
c. Tropospheric rainout time changes	L	L	M	M
d. Sulfuric acid particles grow in troposphere	L	M	L	H
e. Cn concentration changes at tropopause	M	M	L	M
f. Cn size changes at tropopause	L	L	L	L
g. Sedimentation ceases	L	H	H	M
III. Nucleation rate				
a. Heterogeneous nucleation time varies	L	L	L	L
IV. Growth rate				
a. Stratospheric temperature changes	L	H	M	M
b. Stratospheric H_2O changes	L	L	L	L
c. H_2SO_4 vapor pressure changes	L	M	M	M
d. H_2SO_4 sticking coefficient decreases	L	L	L	L
e. Heteromolecular growth ceases	L	H	H	H
f. Coagulation ceases	H	L	L	L
g. Water vapor growth ceases	L	L	L	L

[a]H = highly sensitive: sensitivity study calculations differ more than observed variability.
M = moderately sensitive: sensitivity study calculations differ as much as observed variability.
L = not sensitive: sensitivity study calculations differ less than observed variability.

Page Intentionally Left Blank

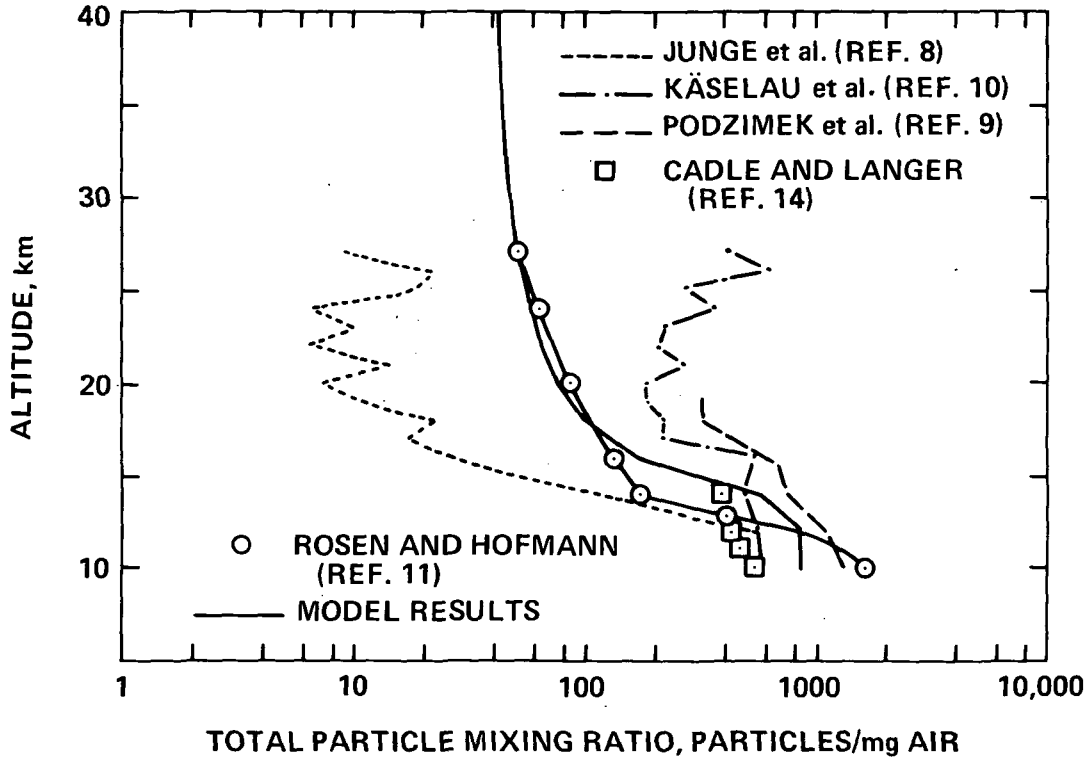

(a) Reference model calculations are compared with observations of the total particle number mixing ratio (all of the particles in 1 mg of air). The data of Junge et al. (ref. 8) average seven measurements; the data of Podzimek et al. (ref. 9) average six measurements; Käselau et al. (ref. 10) average three measurements; and the data of Rosen and Hofmann (ref. 11) also average several measurements. The data were all collected with condensation counters but the experimental equipment, supersaturation, and condensing fluids differed.

Figure 1.– Reference model calculations compared with observations of the stratospheric aerosols.

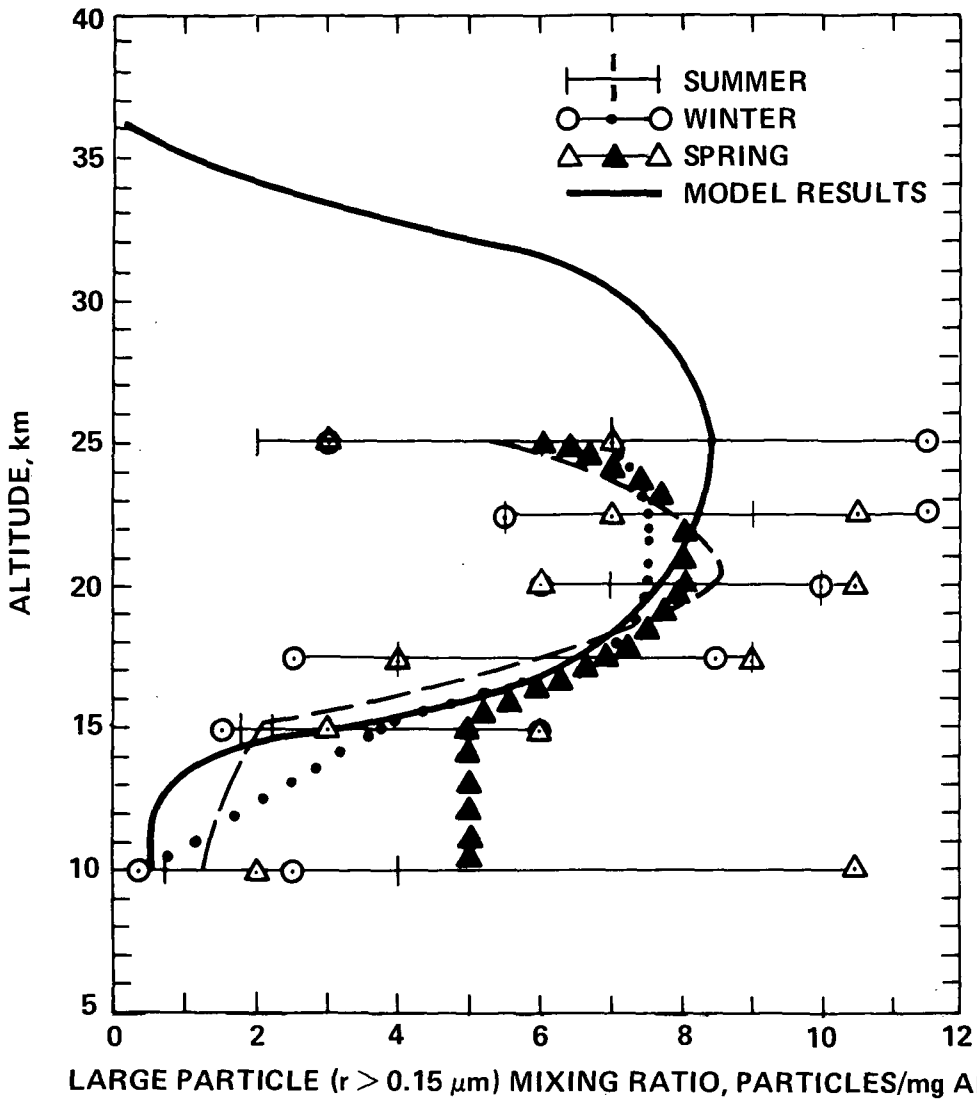

(b) Reference model calculations are compared with observations of the large particle number mixing ratio (all of the particles with $r > 0.15$ μm in 1 mg of air). The measurements were made at northern midlatitudes during 1972-1973 with balloon-borne optical particle counters that discriminated against particles smaller than 0.15 μm (refs. 12, 13). Shown are the mean value of the data and the edge of the envelope containing the individual measurements. Individual measurements show the layer is highly stratified with 50% variations in mixing ratio over 1 km vertical distances. The data have little seasonal trend. A mixing ratio maximum generally occurs around 24 km at the equator and 17 km over the poles. The maximum mixing ratio is 50% greater at the equator than the poles. We chose to illustrate data from 1972-1973 since the total number of particles was near a minimum and the data were thus the least volcanically perturbed data available.

Figure 1.– Continued.

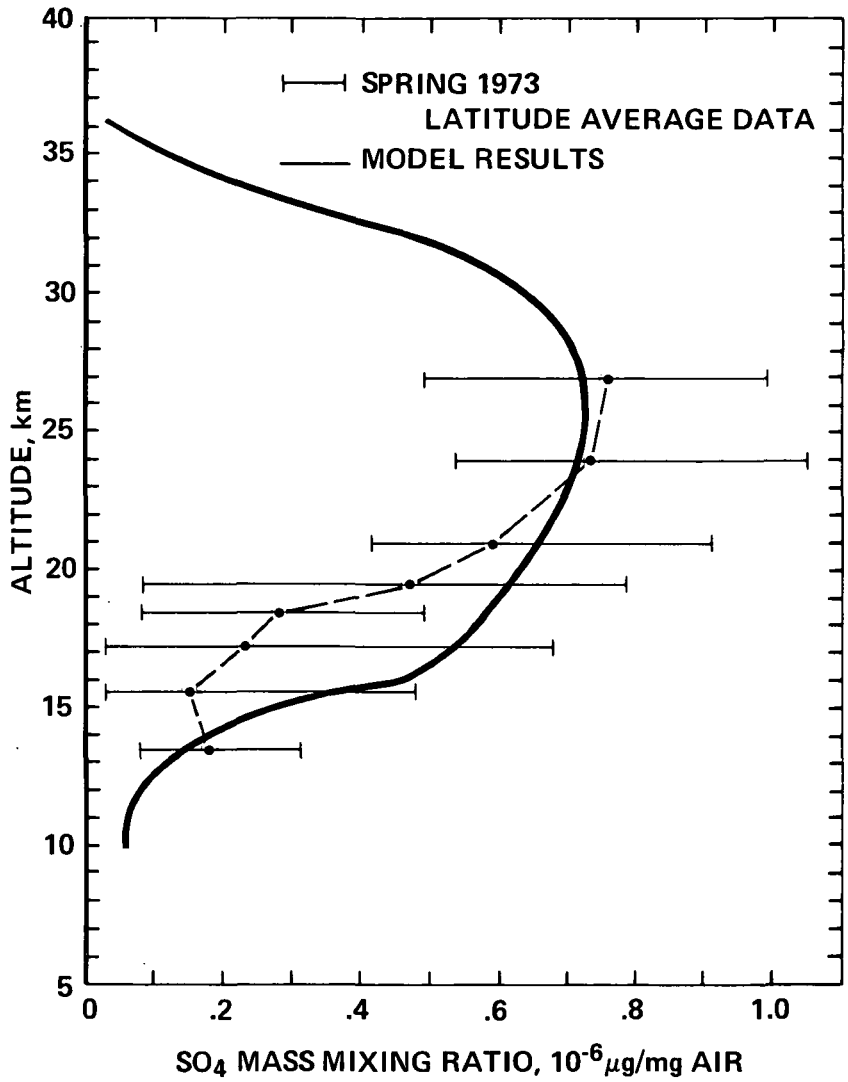

(c) Reference model calculations are compared with observations of the particulate sulfate mass mixing ratio (micrograms of sulfate per miligram of air). The data were obtained by averaging the spring 1973 filter collection data of Lazrus and Gandrud (ref. 15) from pole to pole. The error bars represent extreme values at individual latitudes. The data do not show a clear maximum mixing ratio. The sulfate mass is shown for 1973 to compare with the large particle data of the same period (fig. 1(b)).

Figure 1.– Continued.

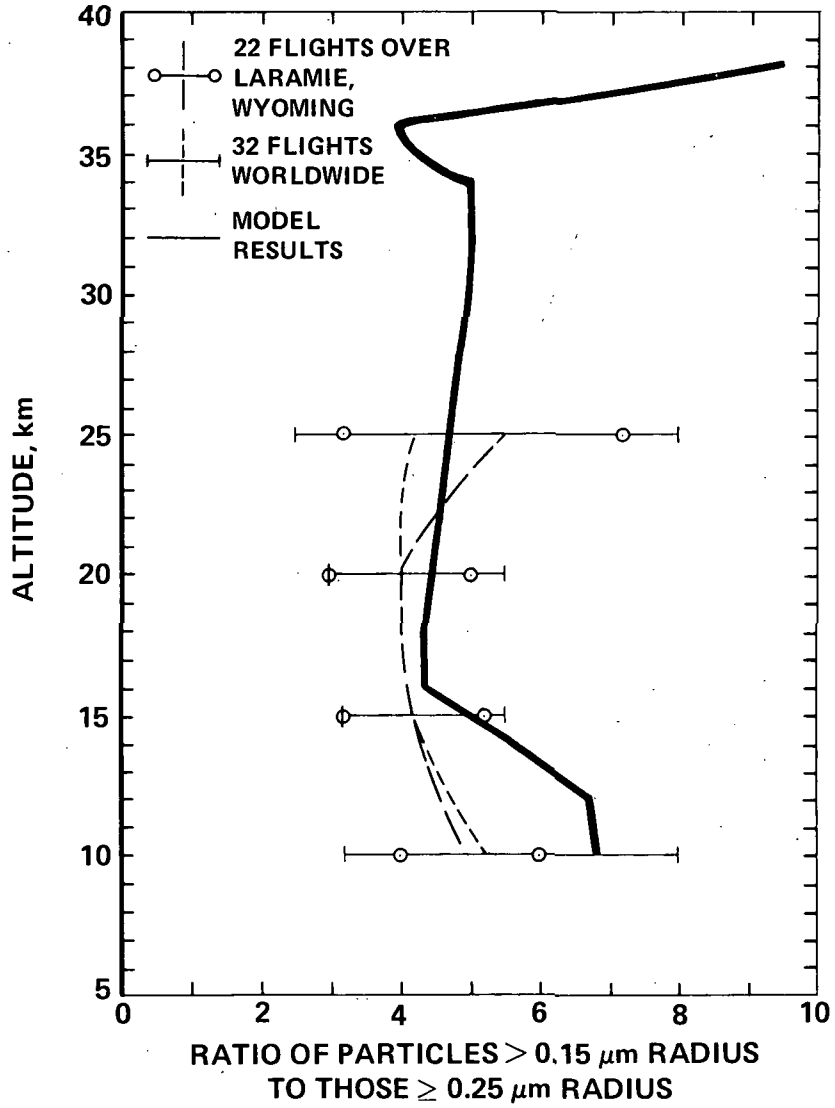

(d) Reference model calculations are compared with observations of the particle size ratio (ratio of the number of particles with $r > 0.15$ μm to the number of particles with $r > 0.25$ μm). These data were taken at several locations from 1971 to 1974 using balloon-borne optical particle counters (ref. 16). Shown are the average values and the envelope containing the individual measurements. The size ratio is quite uniform in time and space.

Figure 1.– Continued.

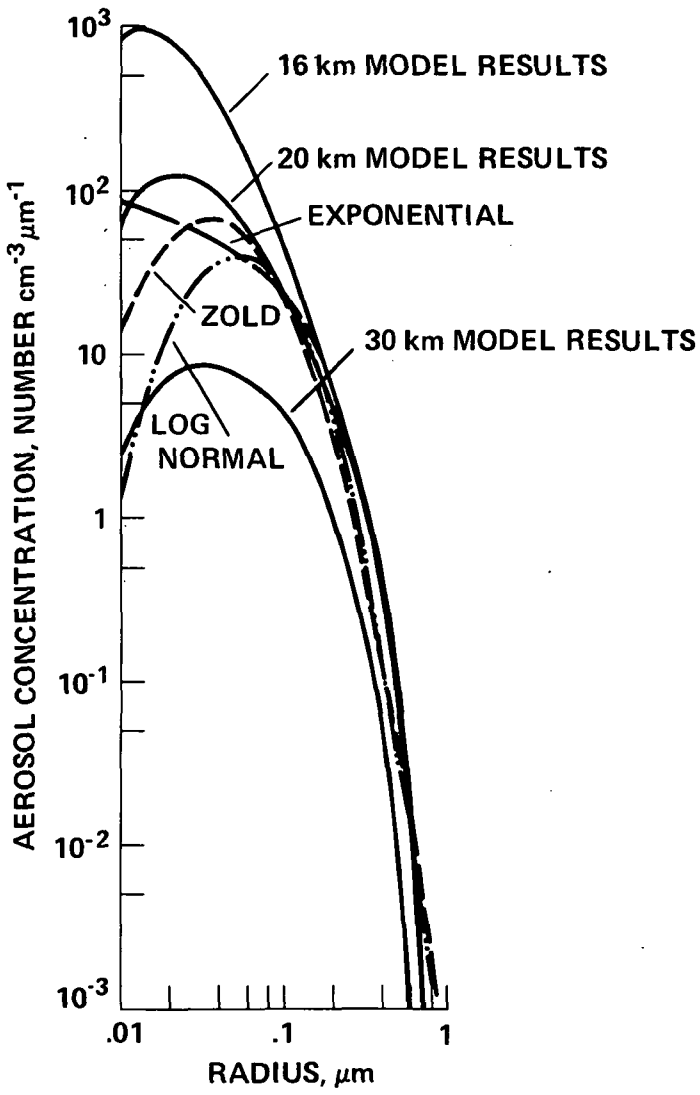

(e) Reference model calculations are compared with observations of the particle size distribution. Toon and Pollack (ref. 17) and Pinnick et al. (ref. 16) compared optical data for large particles, Cn measurements, and impactor data to find average stratospheric size distributions. Above 0.1 μm, the size distribution is not a strong function of altitude and the shape of the zero order logarithmic distribution (ZOLD) (ref. 17) compares well with the shape of the exponential and the log-normal distributions (ref. 16). Below 0.1 μm, the size distribution appears to be a strong function of altitude (fig. 1(a) compared to 1(b)). All three empirical size distributions are equally compatible with the available data at 20 km and no single distribution can be used as an altitude average.

Figure 1.– Concluded.

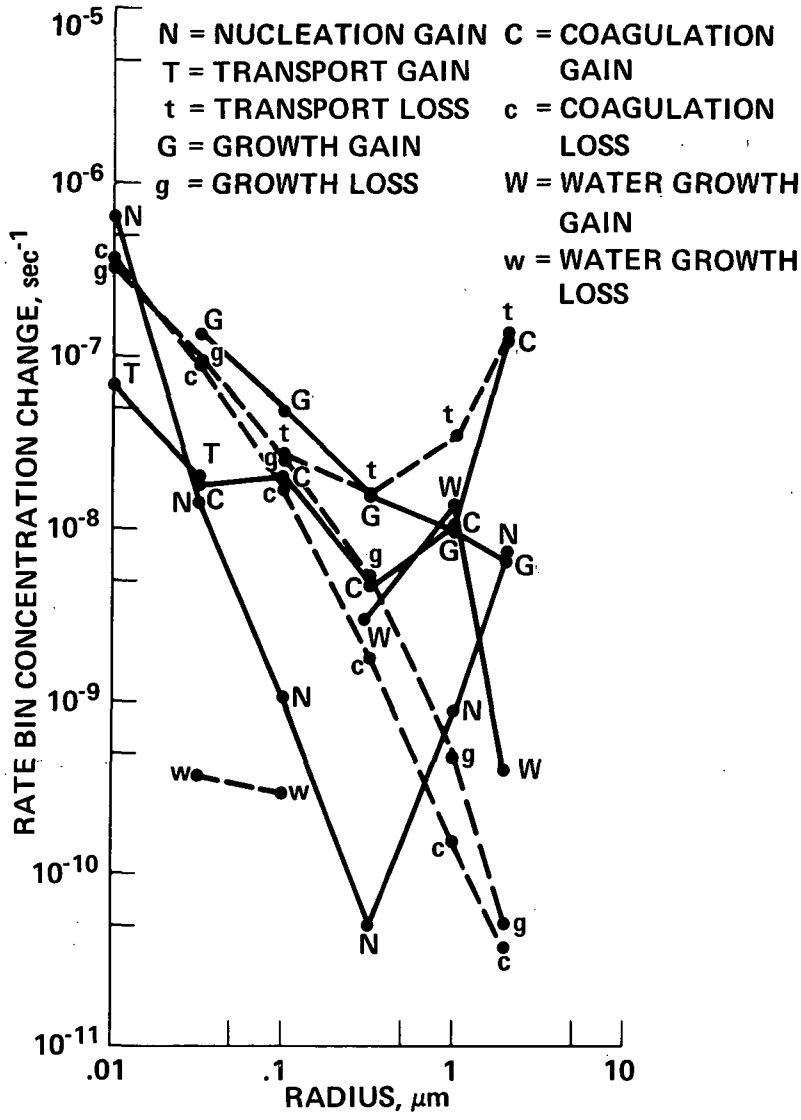

(a) 16-km altitude.

Figure 2.– The rate at which the aerosol droplet size bins in the reference model are filled (solid) lines) or emptied (dashed lines) by the physical processes in our model at altitudes of 16 km, 20 km, and 30 km.

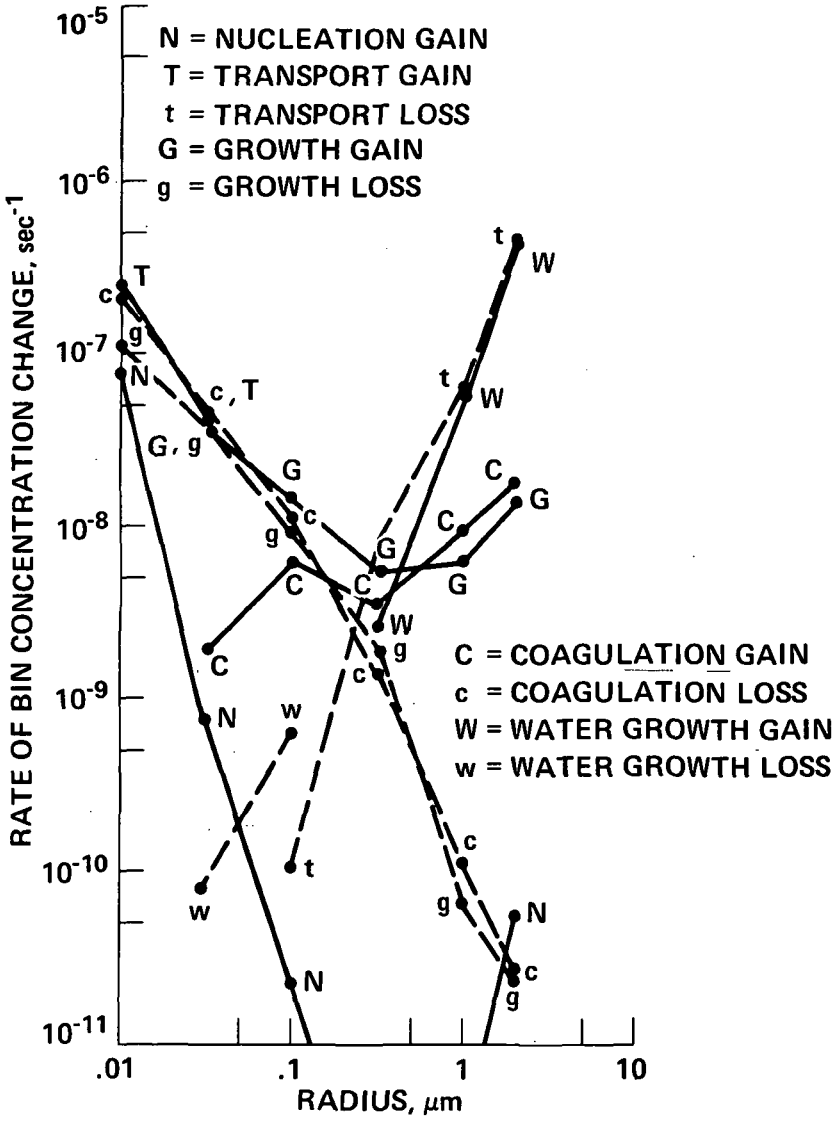

(b) 20-km altitude.

Figure 2.– Continued.

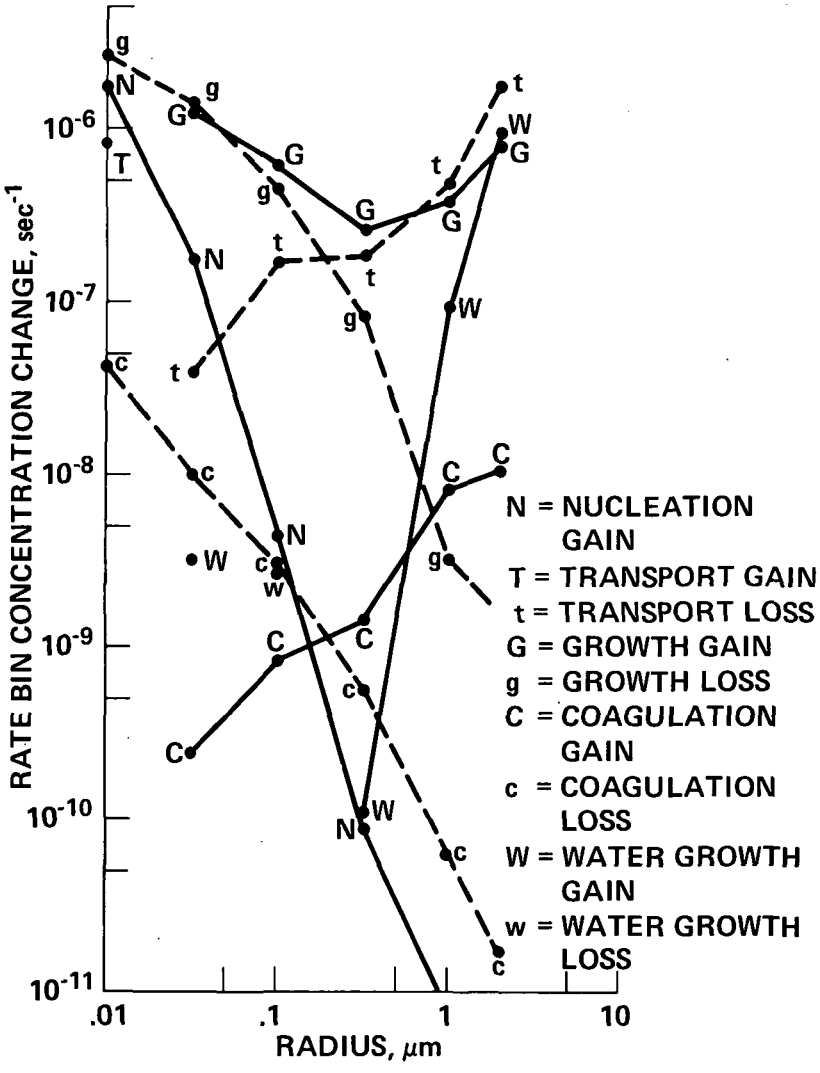

(c) 30-km altitude.

Figure 2.– Concluded.

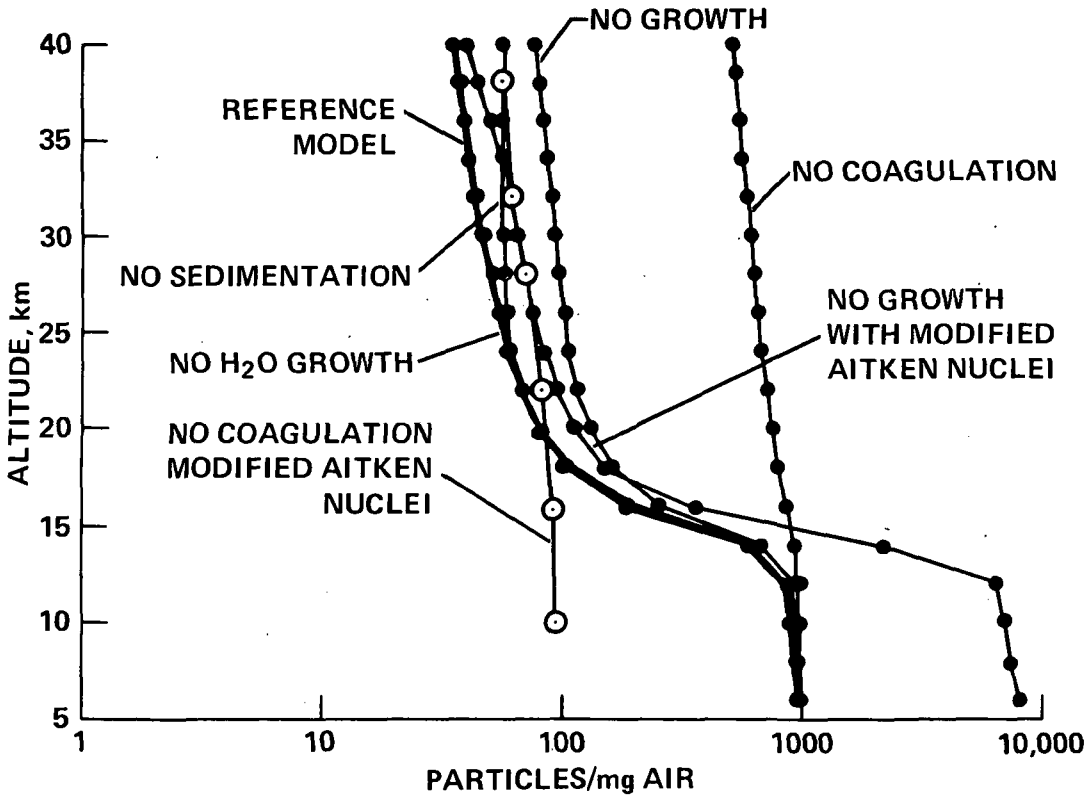

(a) Total particle mixing ratio.

Figure 3.– Reference model calculations are compared with model calculations in which various physical processes are omitted.

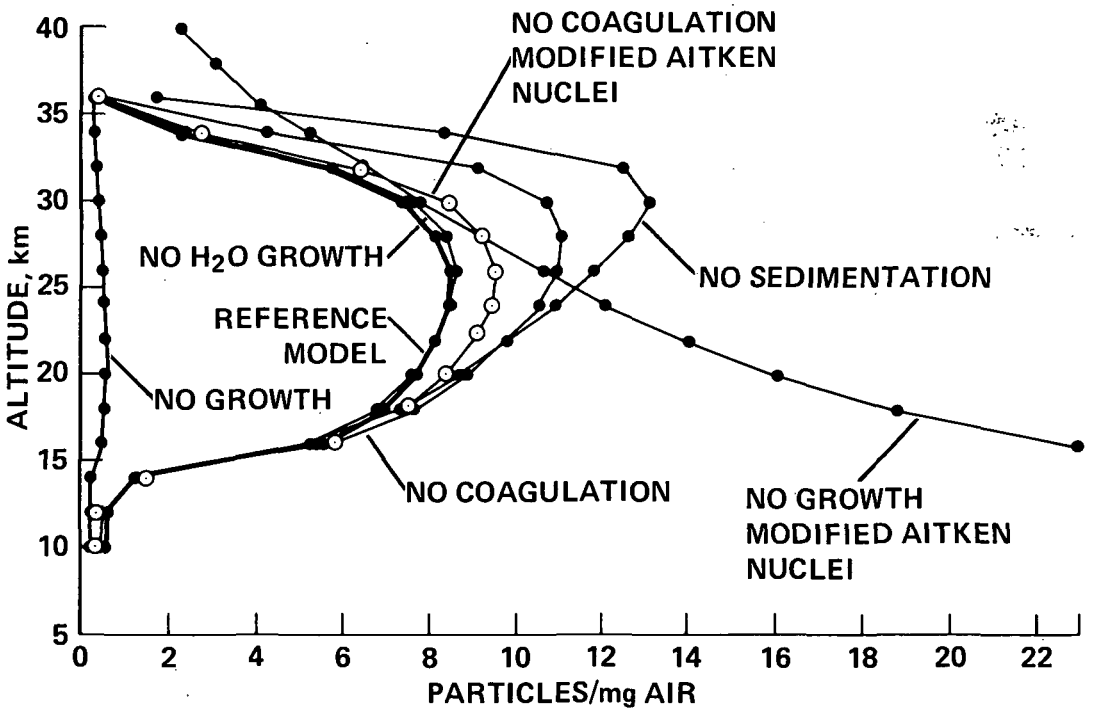

(b) Large particle ($r > 0.15$ μm) mixing ratio.

Figure 3.– Continued.

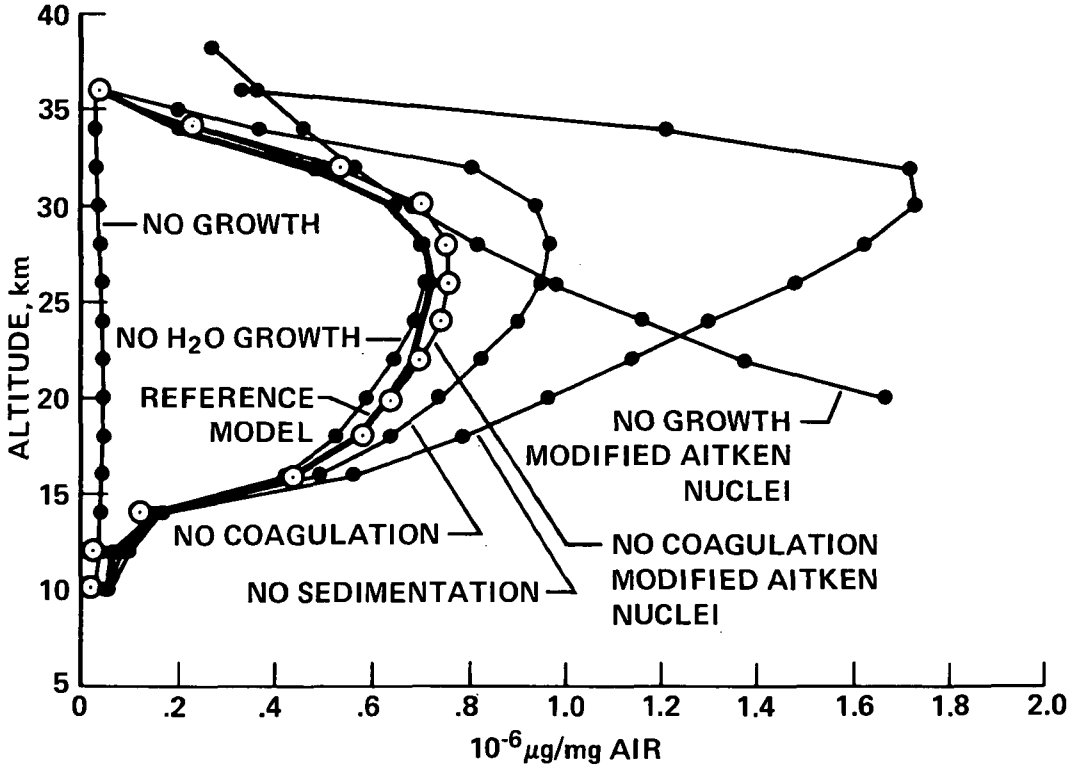

(c) SO_4 mass mixing ratio.

Figure 3.– Continued.

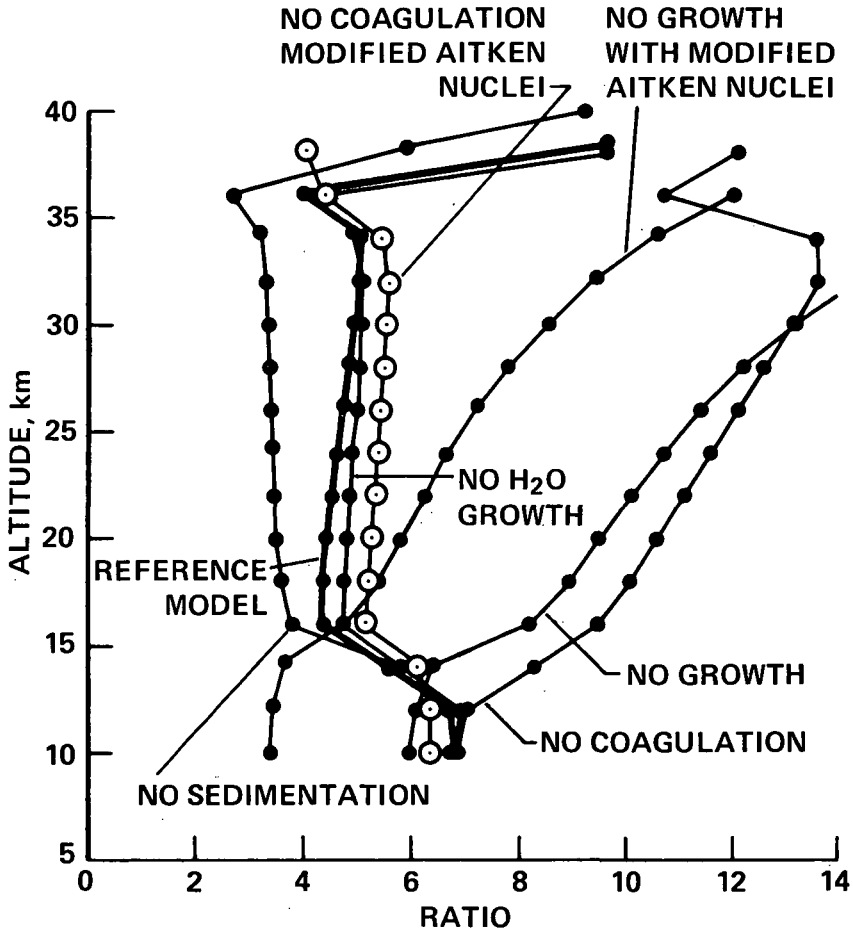

(d) Ratio of particles $\geqslant 0.15$ μm radius to those $\geqslant 0.25$ μm radius.

Figure 3.– Concluded.

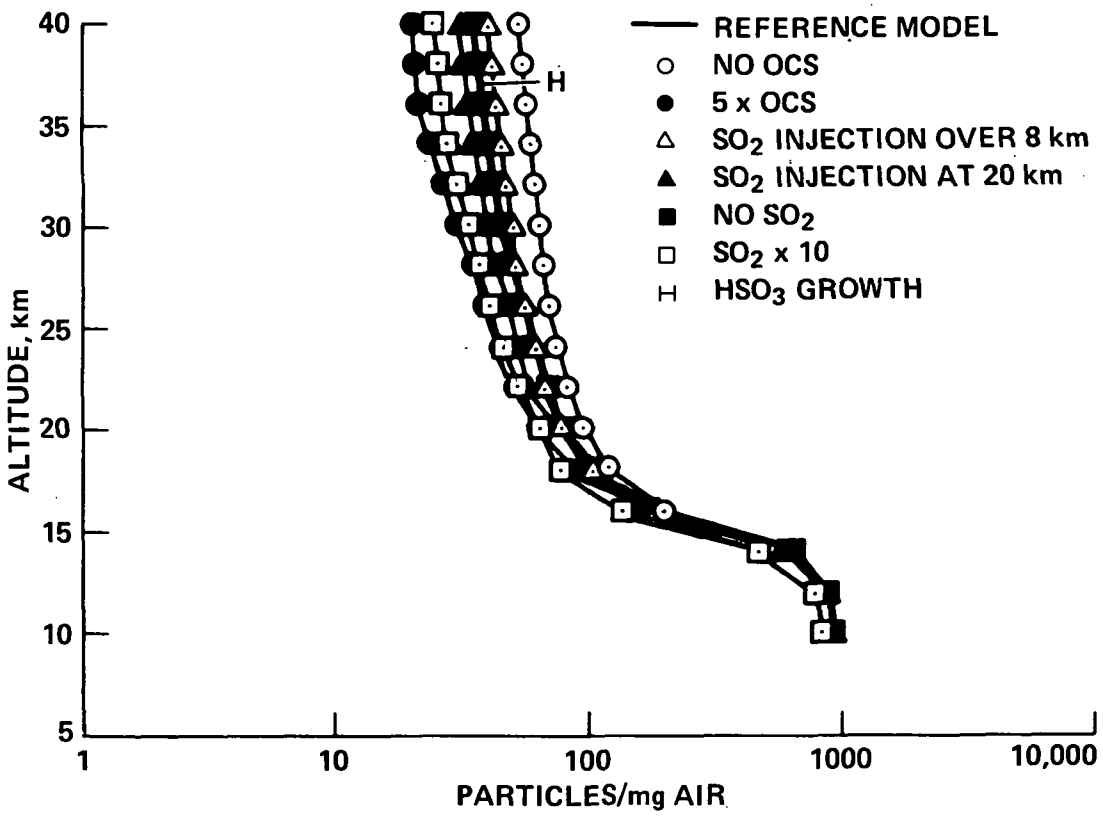

(a) Total particle mixing ratio.

Figure 4.– Reference model calculations are compared with model calculations in which the sulfur gas supply is altered.

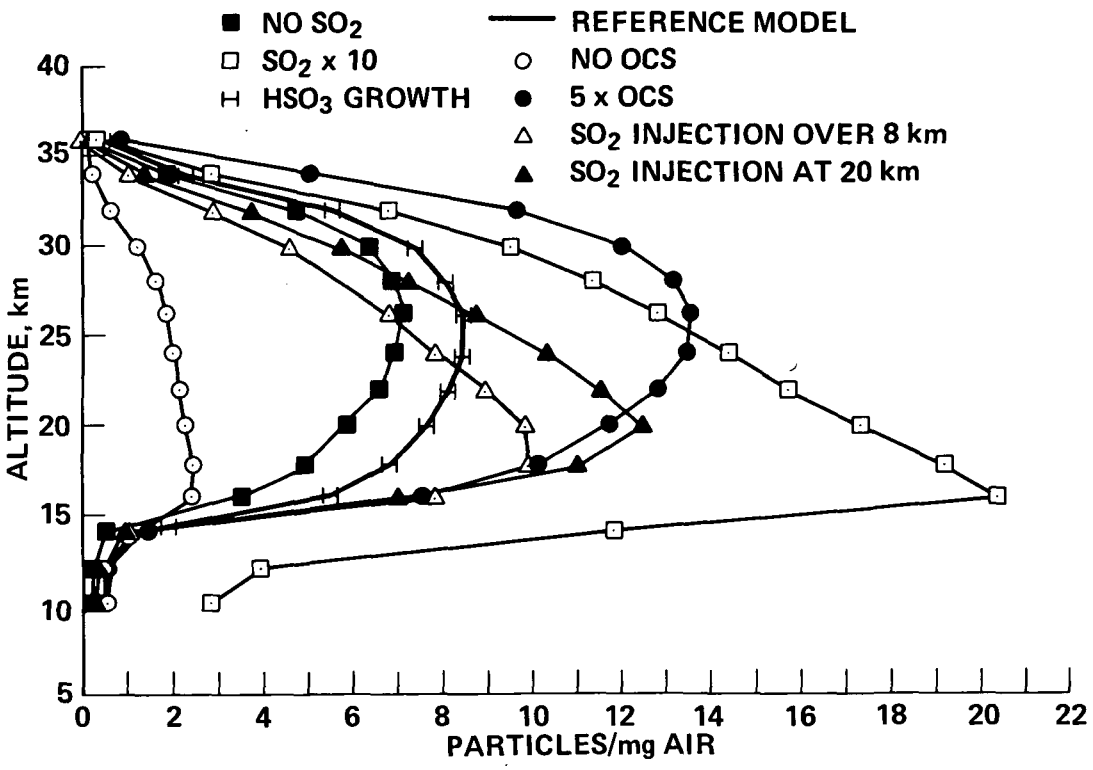

(b) Large particle ($r > 0.15$ μm) mixing ratio.

Figure 4.– Continued.

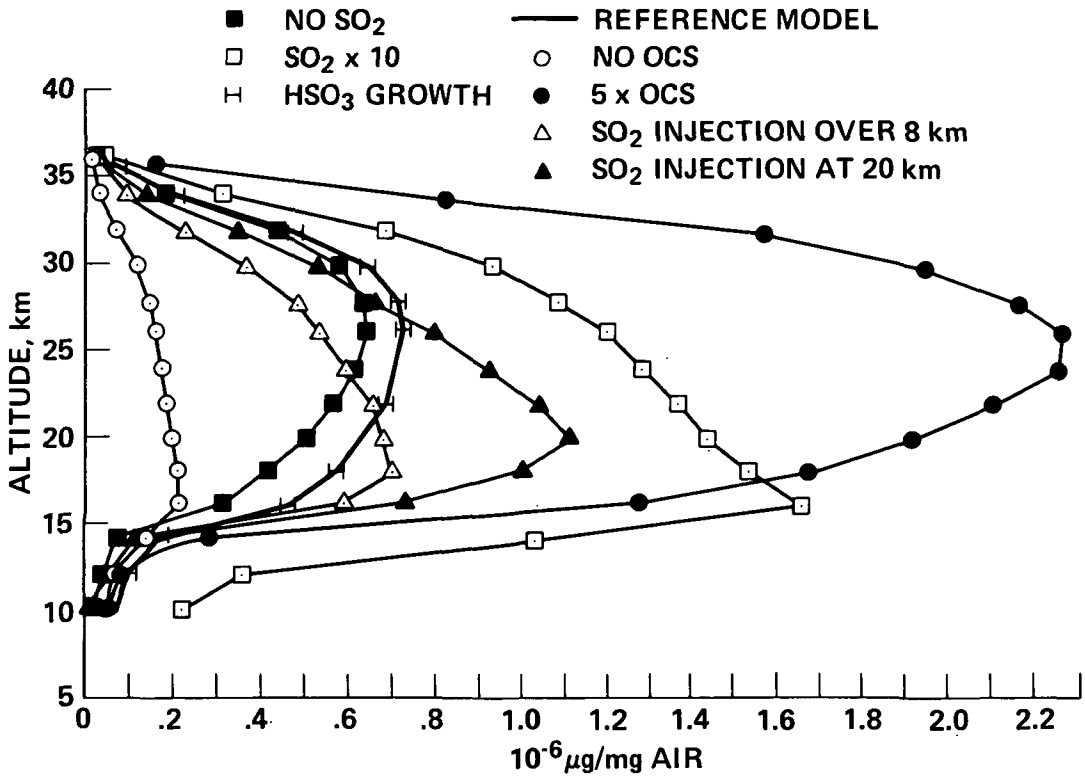

(c) SO_4 mass mixing ratio.

Figure 4.– Continued.

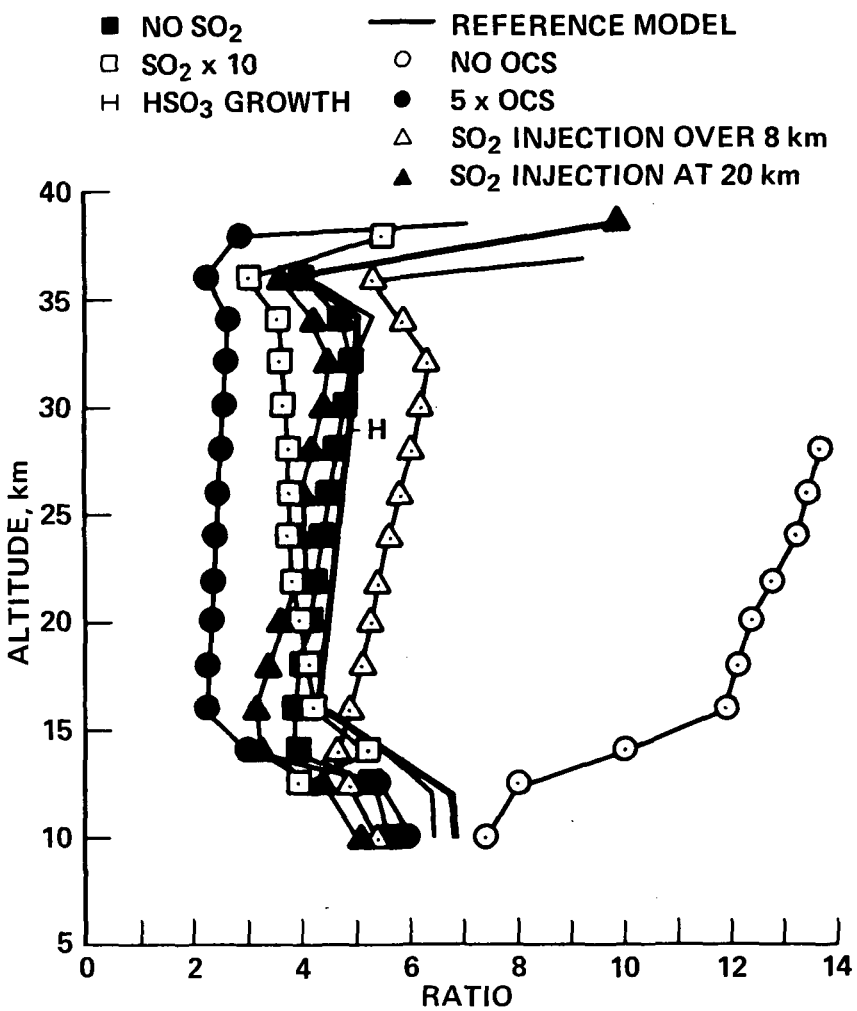

(d) Ratio of particles $\geqslant 0.15$ μm radius to those $\geqslant 0.25$ μm radius.

Figure 4.– Concluded.

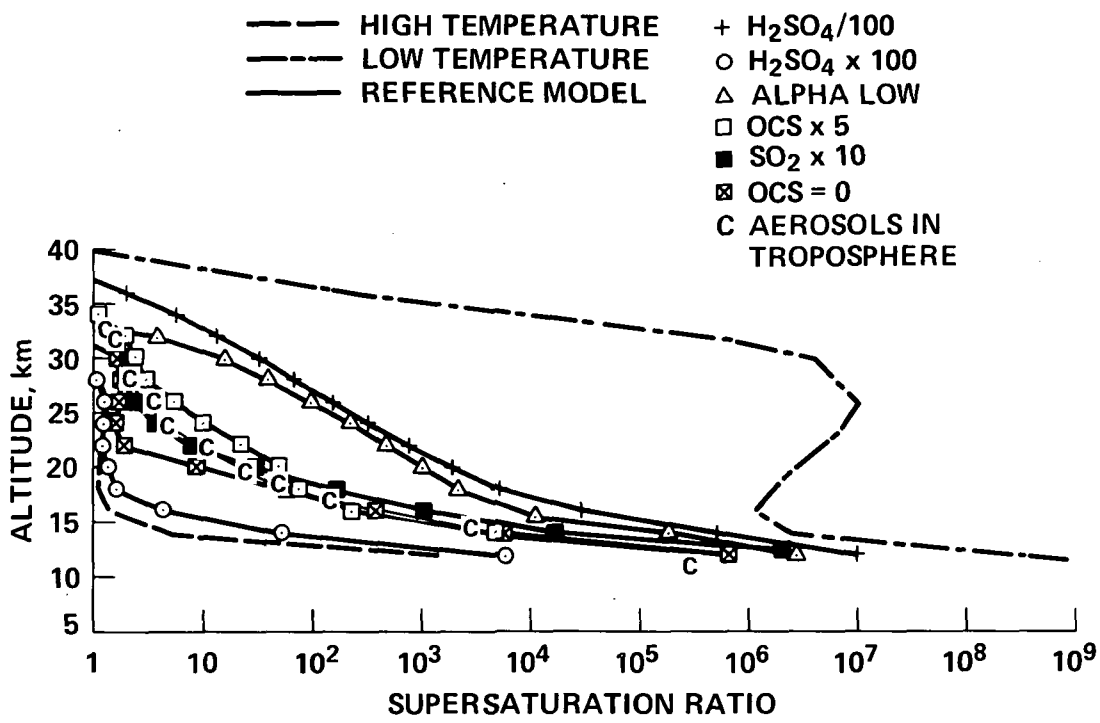

Figure 5.– The H_2SO_4 supersaturation, or ratio of H_2SO_4 partial pressure to H_2SO_4 vapor pressure (over a flat surface), for a number of calculations in which various parameters in the model have been changed. The reference model curve is nearly indistinguishable from the curve labeled *C*.

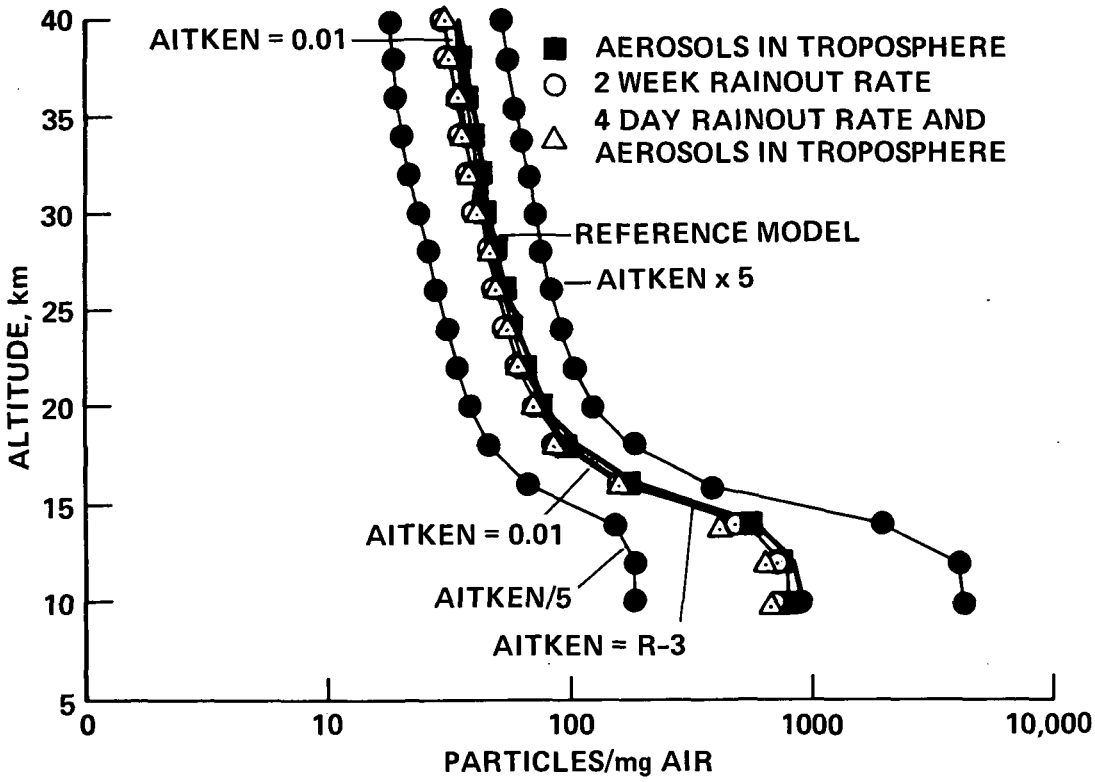

(a) Total particle mixing ratio.

Figure 6.– Reference model calculations are compared with calculations in which the properties of the upper tropospheric aerosols (Cn, Aitken nuclei) are altered.

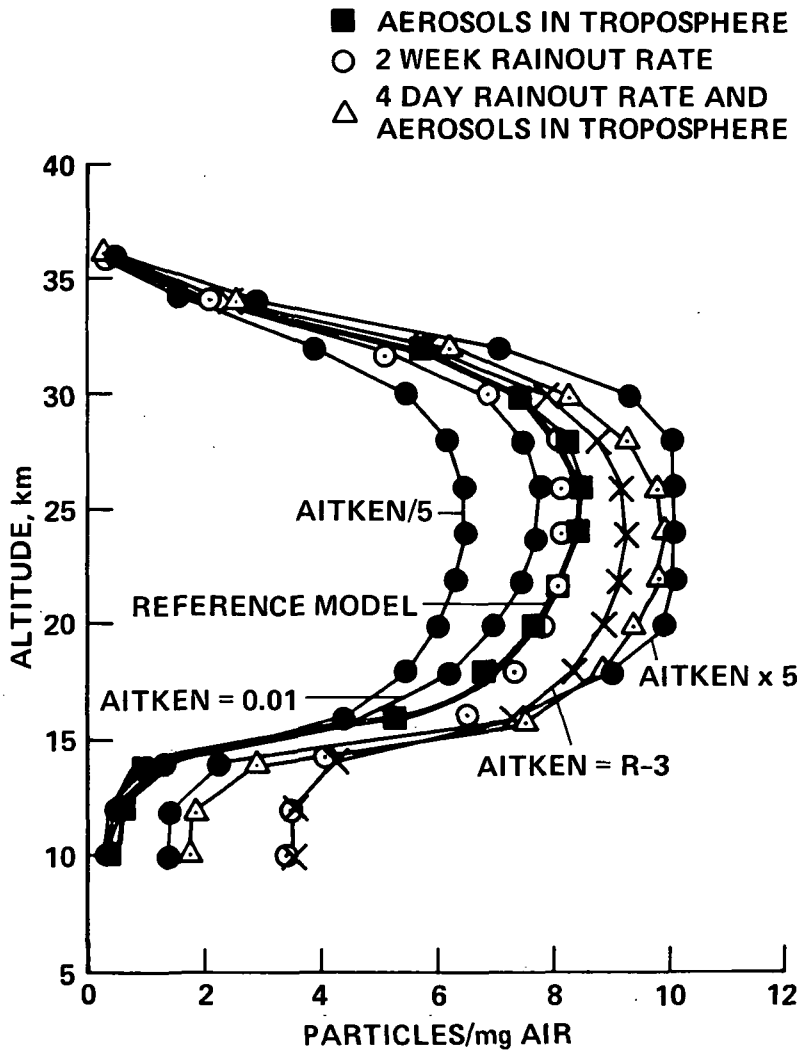

(b) Large particle ($r > 0.15$ μm) mixing ratio.

Figure 6.– Continued.

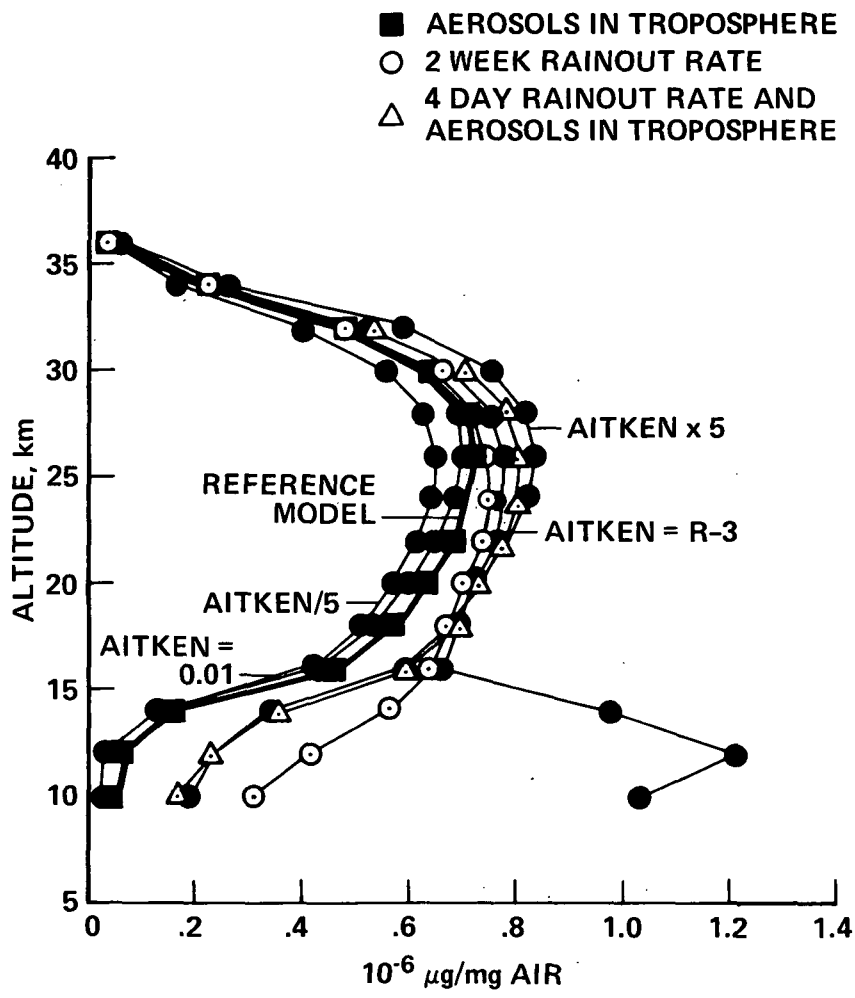

(c) SO_4 mass mixing ratio.

Figure 6.– Continued.

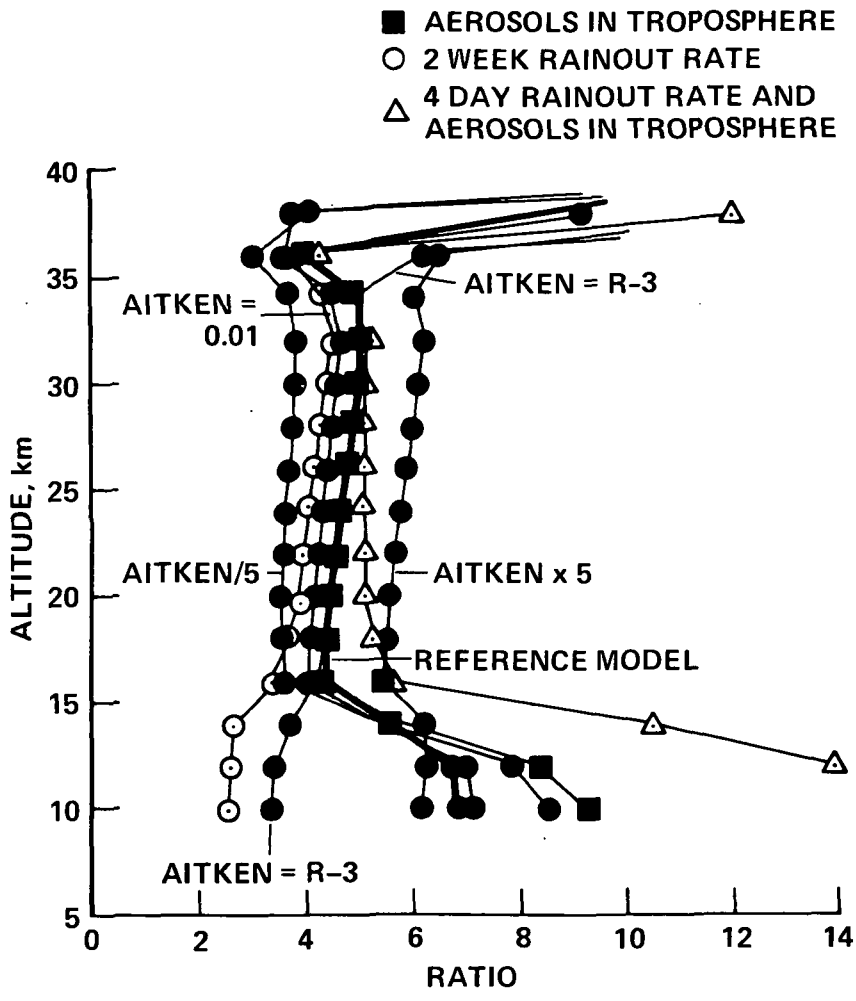

(d) Ratio of particles $\geqslant 0.15$ μm radius to those $\geqslant 0.25$ μm radius.

Figure 6.– Concluded.

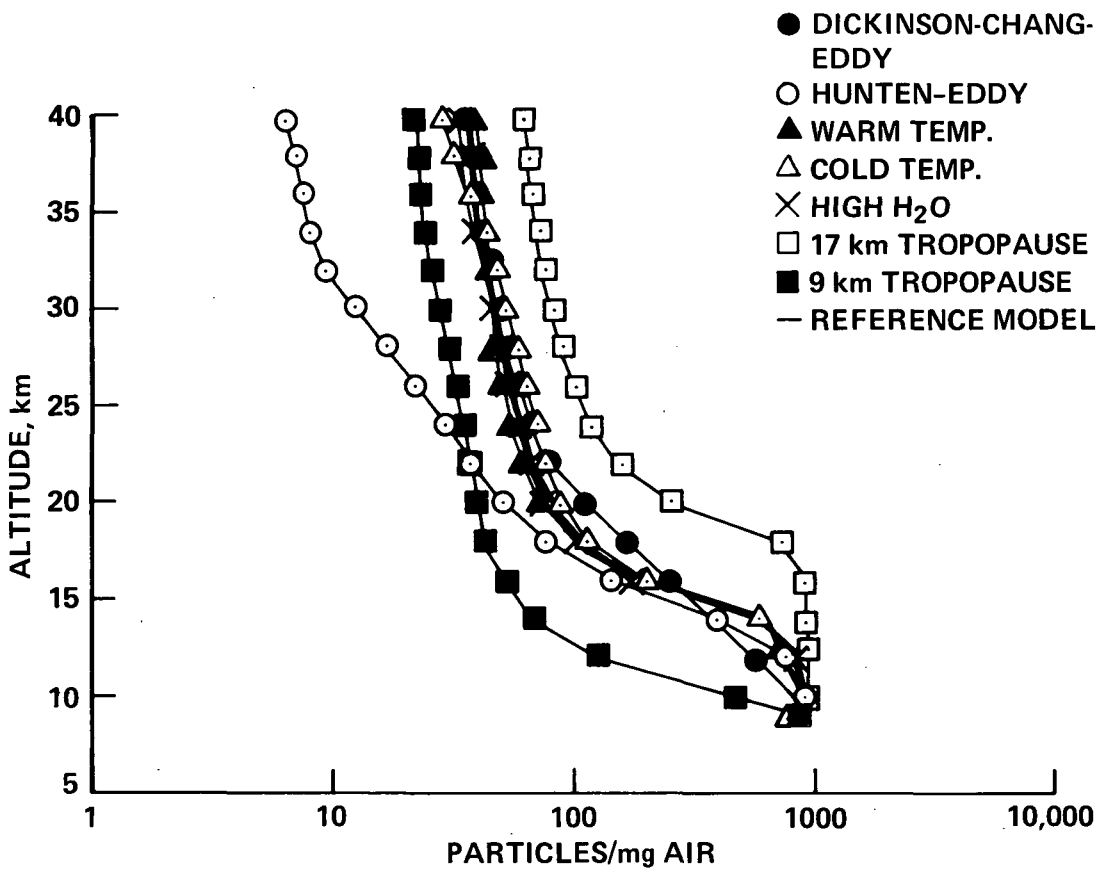

(a) Total particle mixing ratio.

Figure 7.– Reference model calculations are compared with calculations in which parameters influencing residence time and factors that undergo natural changes are altered.

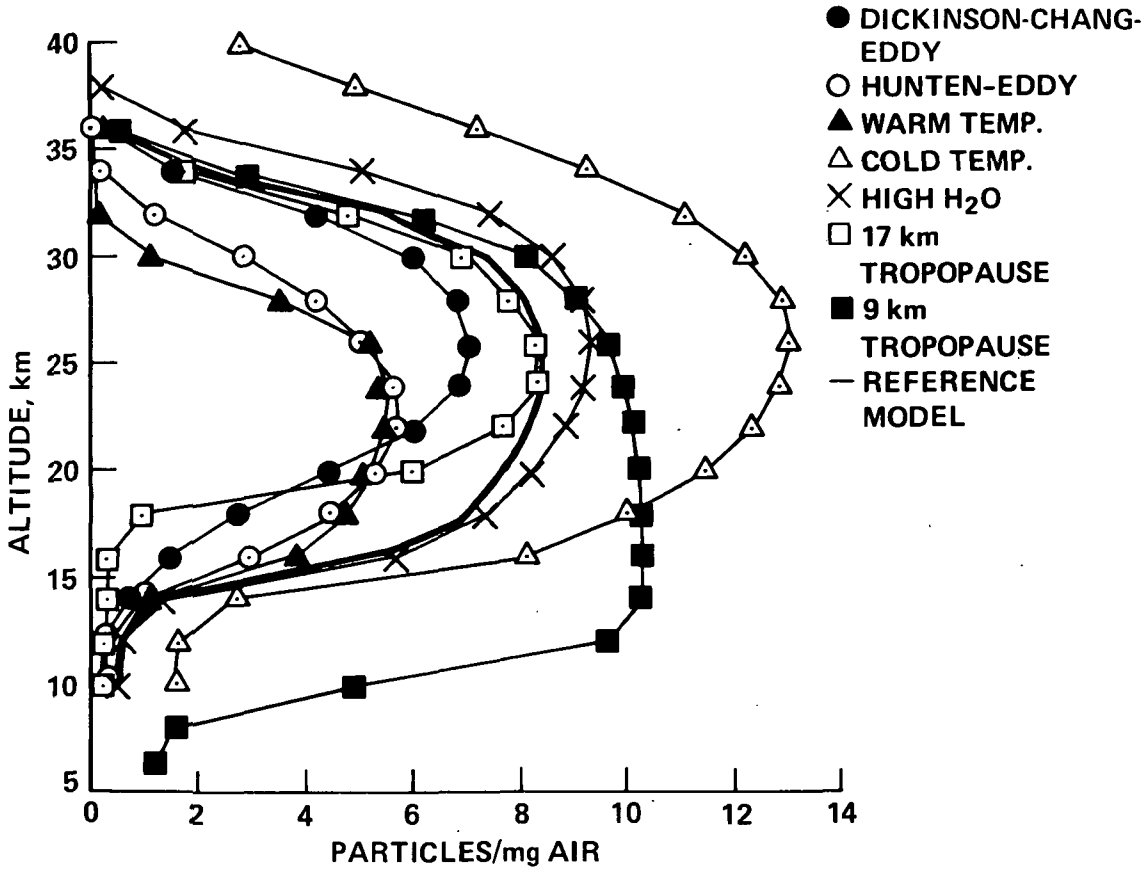

(b) Large particle ($r > 0.15$ μm) mixing ratio.

Figure 7.– Continued.

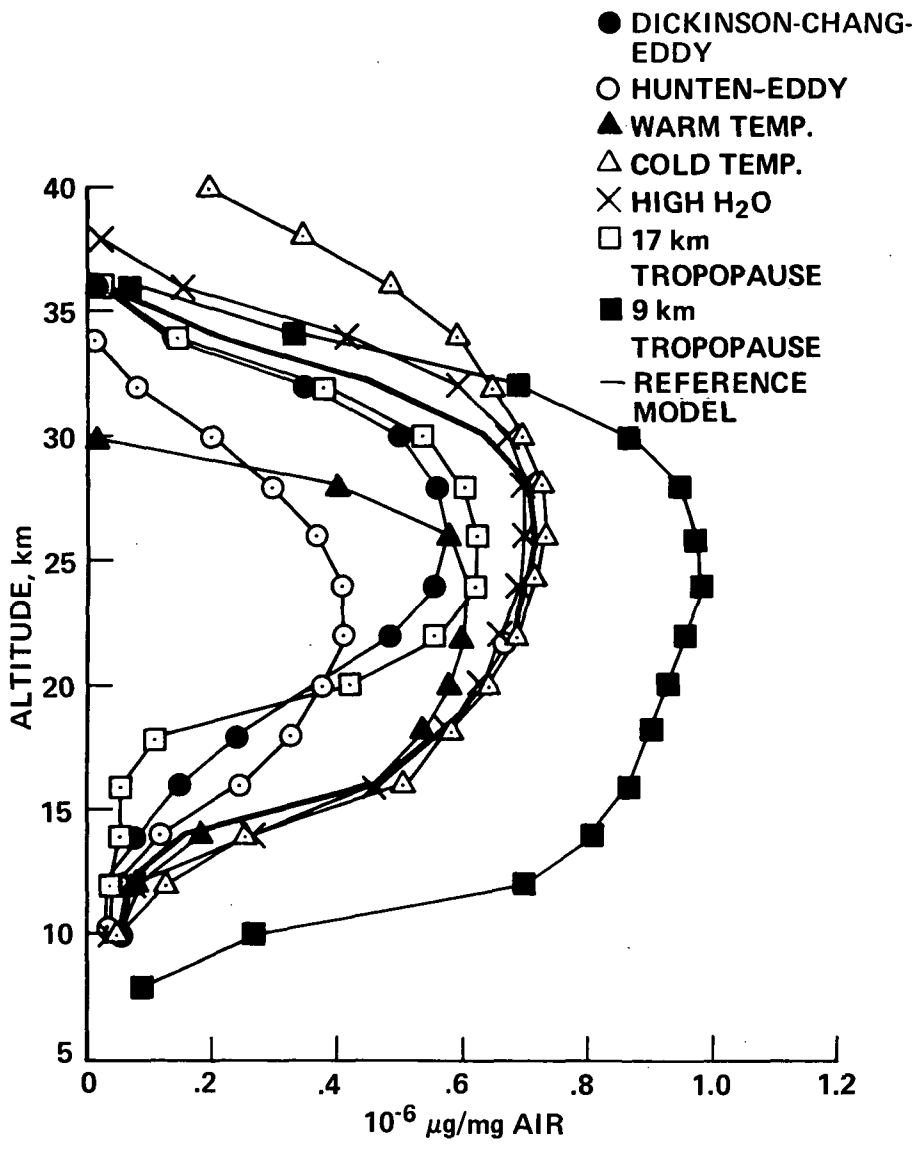

(c) SO_4 mass mixing ratio.

Figure 7.– Continued.

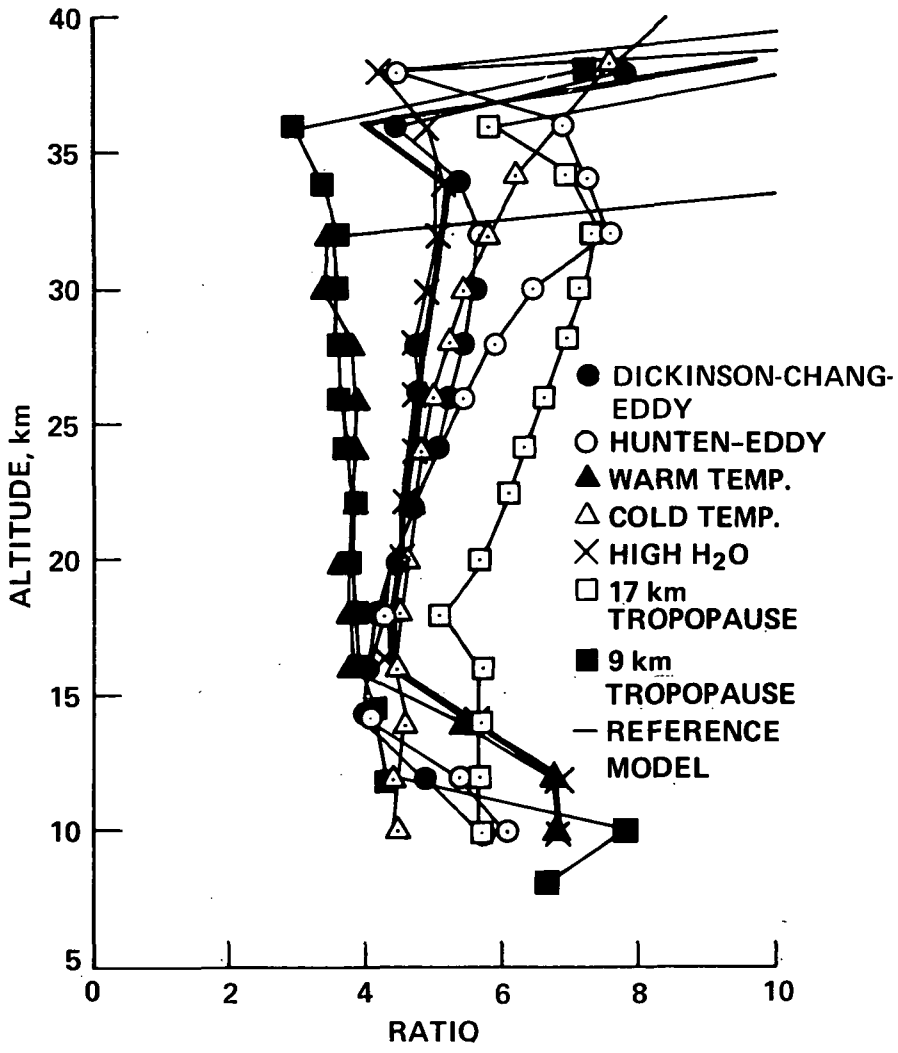

(d) Ratio of particles $\geqslant 0.15$ μm radius to those $\geqslant 0.25$ μm radius.

Figure 7.– Concluded.

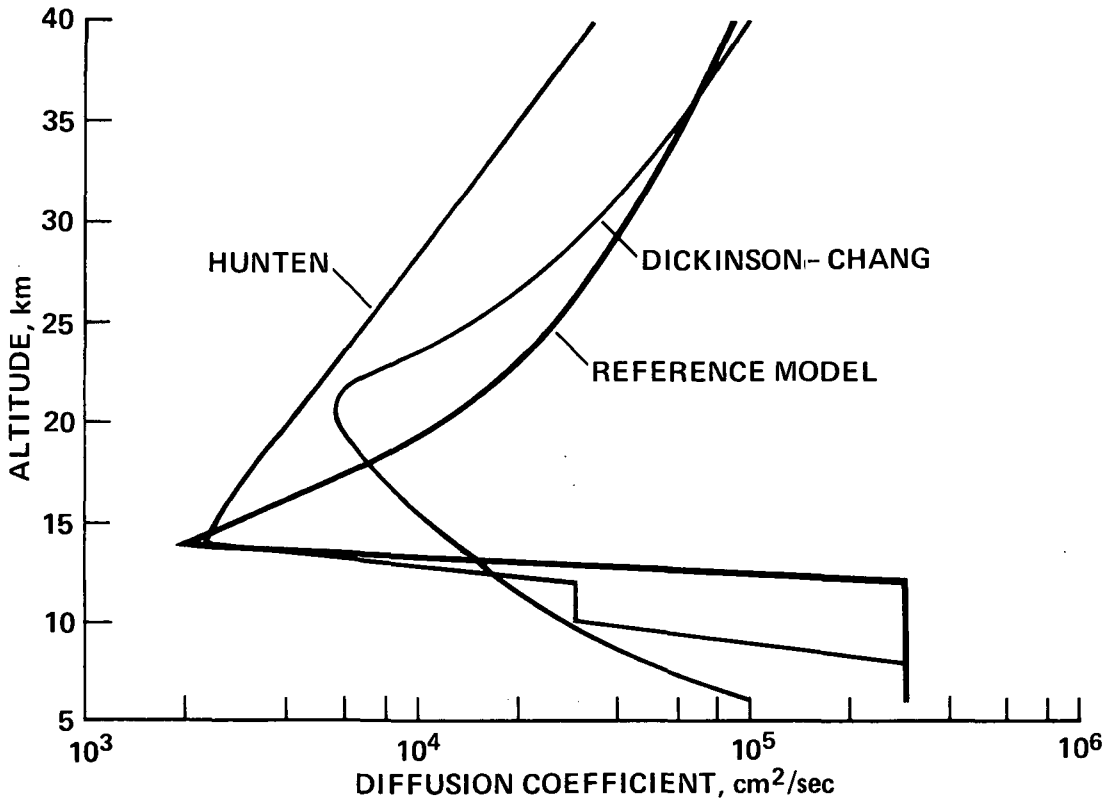

Figure 8.– Reference model and alternate diffusion coefficient profiles are compared.

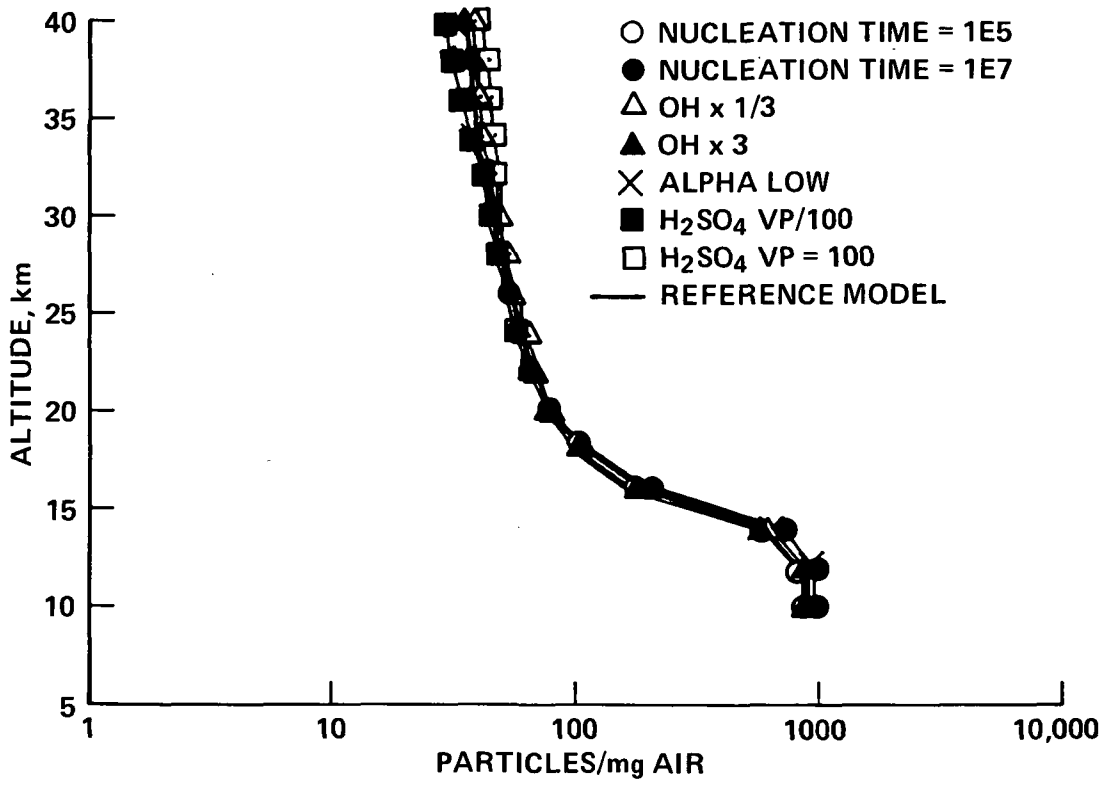

(a) Total particle mixing ratio.

Figure 9.– Reference model calculations are compared with calculations in which poorly known, or unmodeled, parameters are altered.

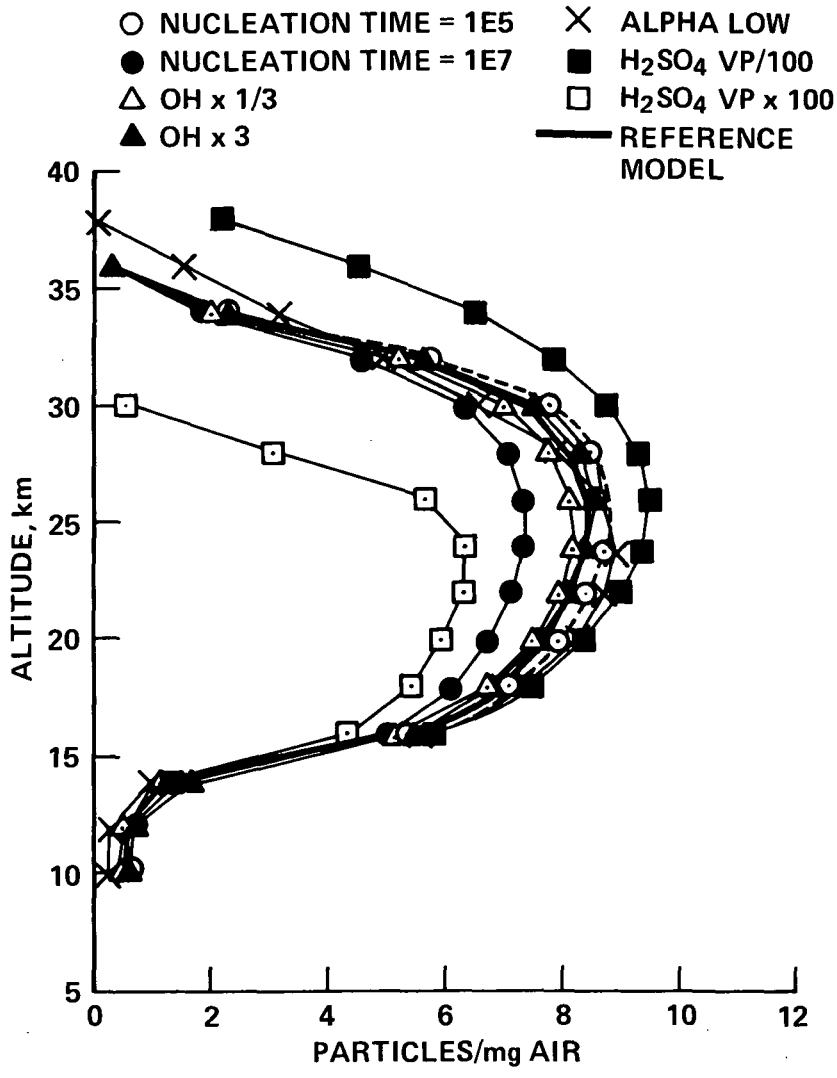

(b) Large particle ($r > 0.15$ μm) mixing ratio.

Figure 9.– Continued.

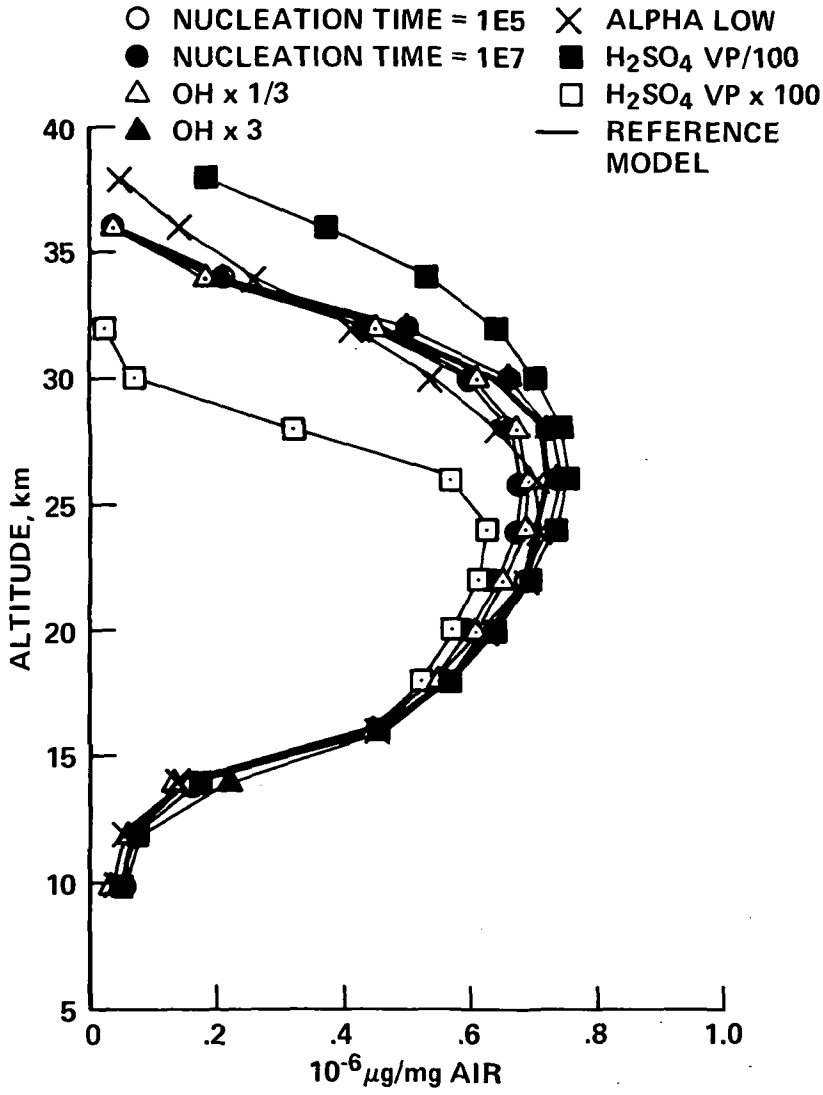

(c) SO_4 mass mixing ratio.

Figure 9.– Continued.

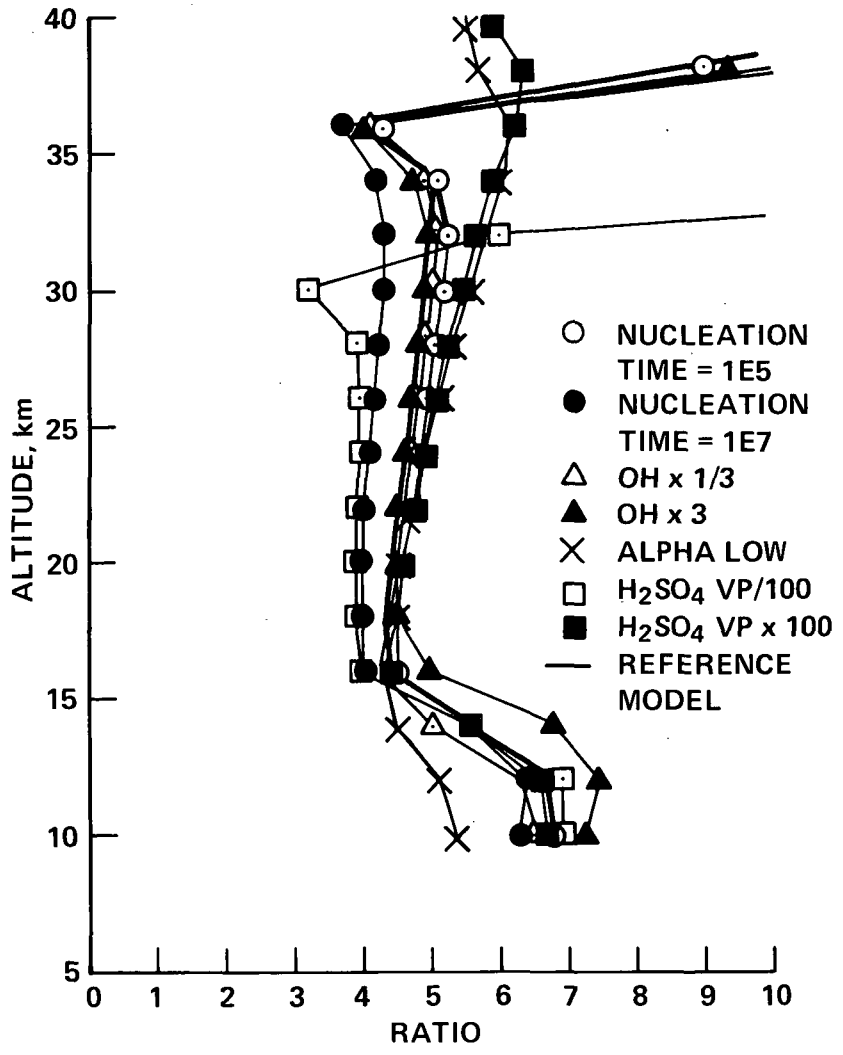

(d) Ratio of particles $\geqslant 0.15$ μm radius to those $\geqslant 0.25$ μm radius.

Figure 9.– Concluded.

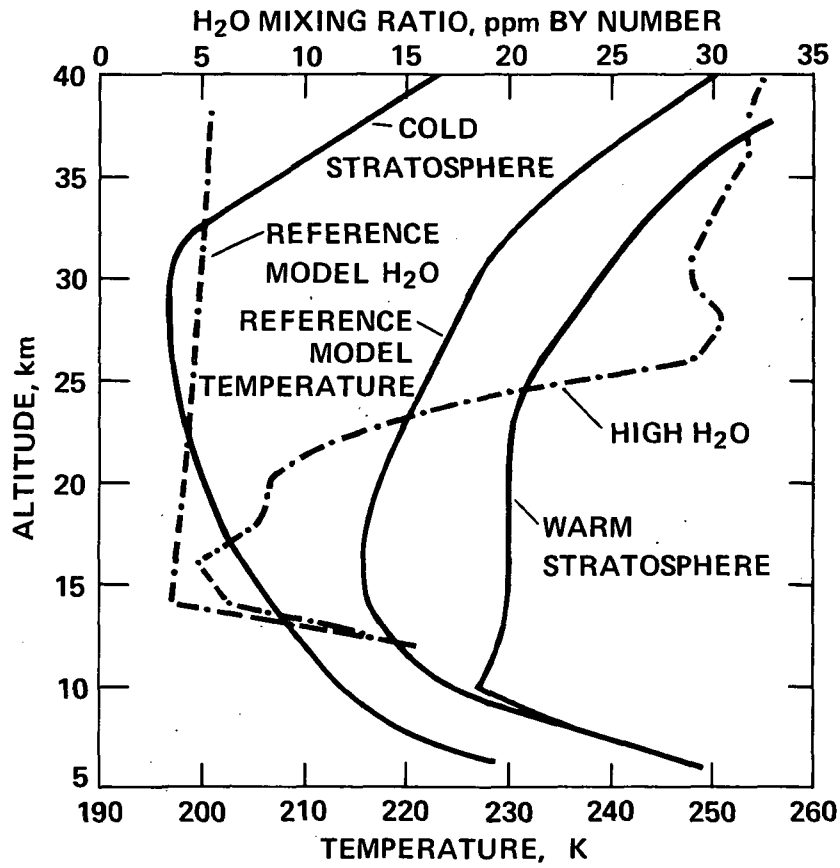

Figure 10.– Reference model temperatures and H_2O mixing ratio profiles are compared with alternate profiles.

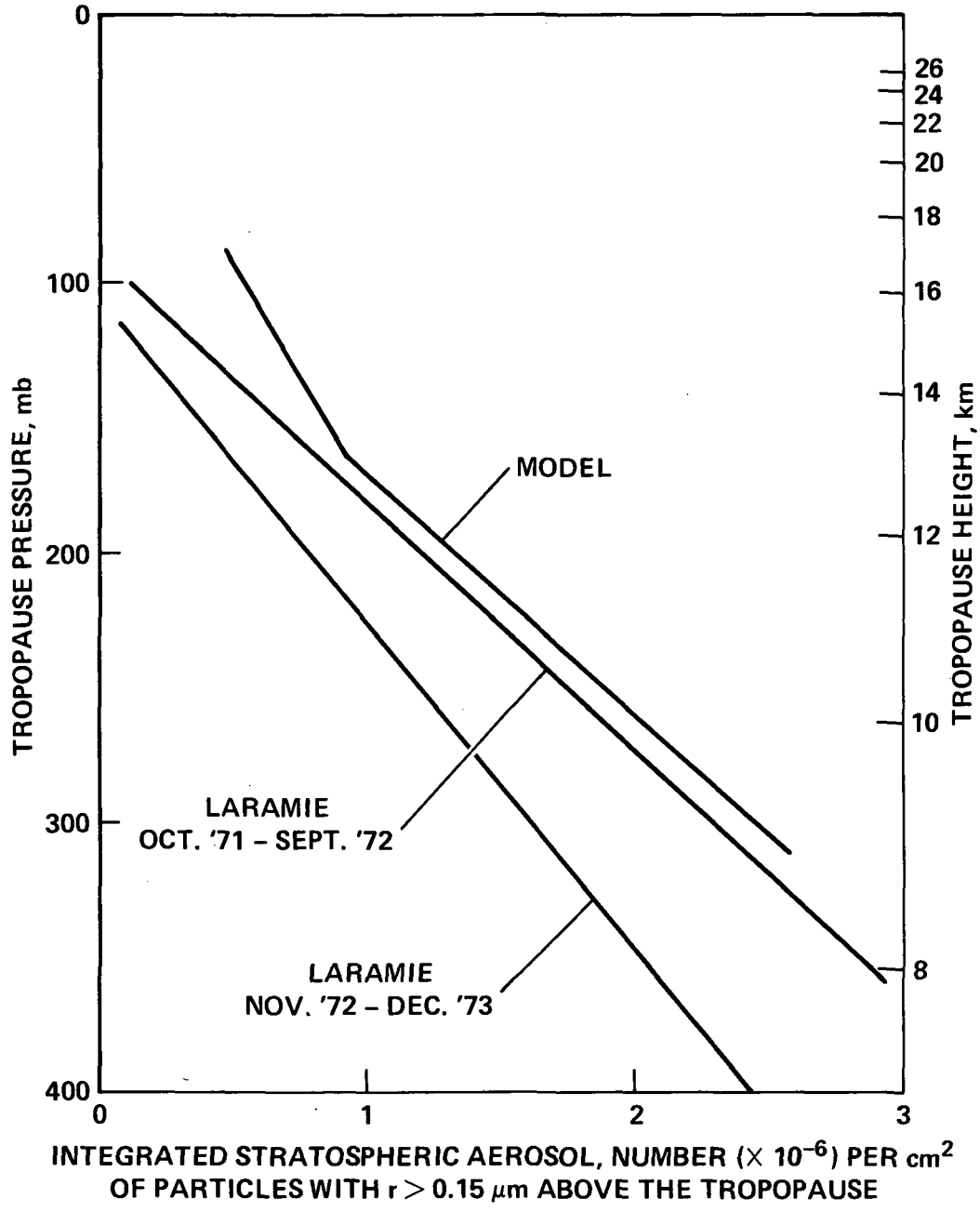

Figure 11.– Observed dependence on tropopause pressure of the total number of large particles above the tropopause compared with calculations in which the tropopause height is varied (see fig. 7). The number of large particles above the tropopause was determined by Hofmann *et al.* (ref. 12) by integrating data such as those shown in figure 1(b) above the tropopause. The difference in figure 11 between the 1971-72 data and the 1972-73 data is probably due to decreasing sulfur gas source strength. Our model profile in figure 11 may be higher than the observations partly because we have large particles extending to greater altitudes than are normally reached in the balloon flights used to gather the data.

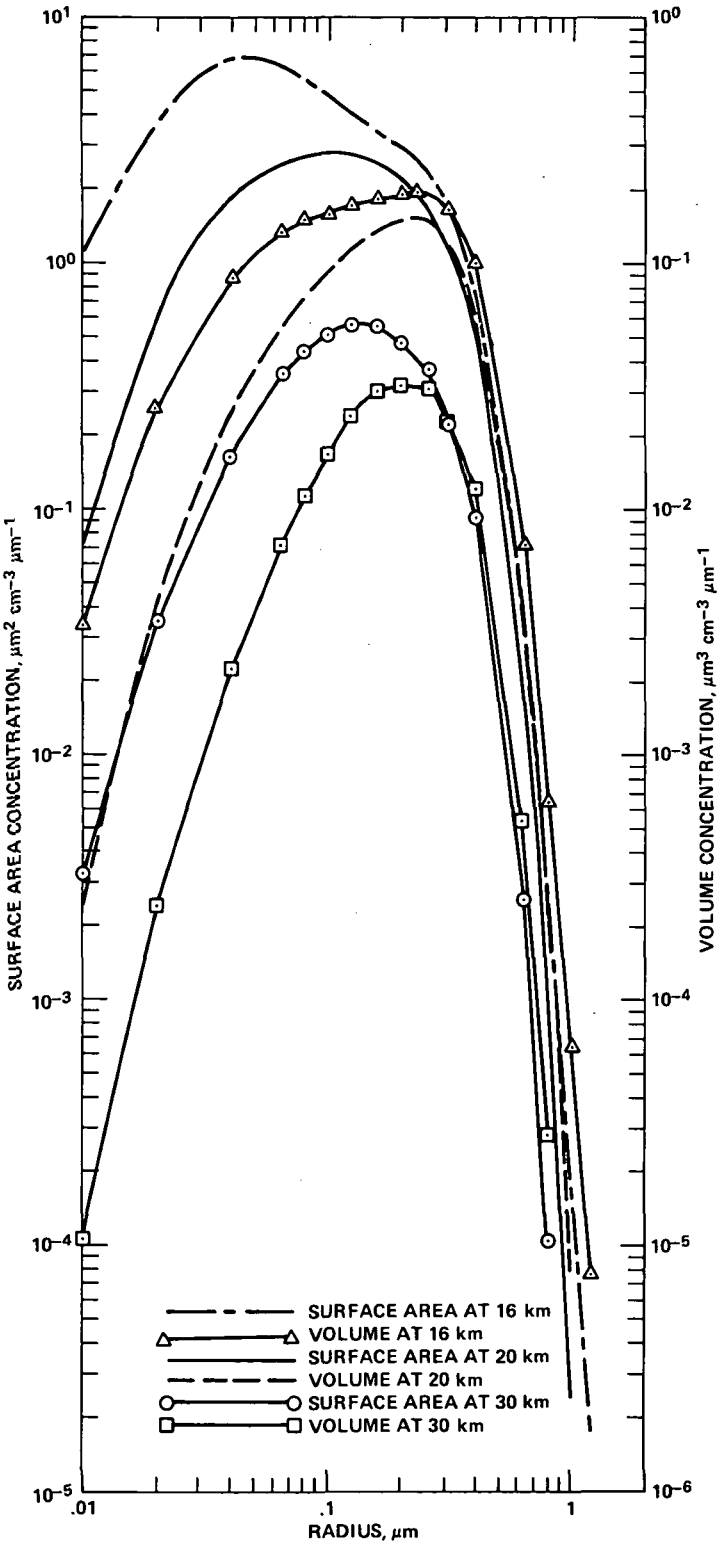

Figure 12.– Reference model calculations of the size distributions by area and volume at 16-, 20-, and 30-km altitudes. The left scale refers to area and the right to volume.

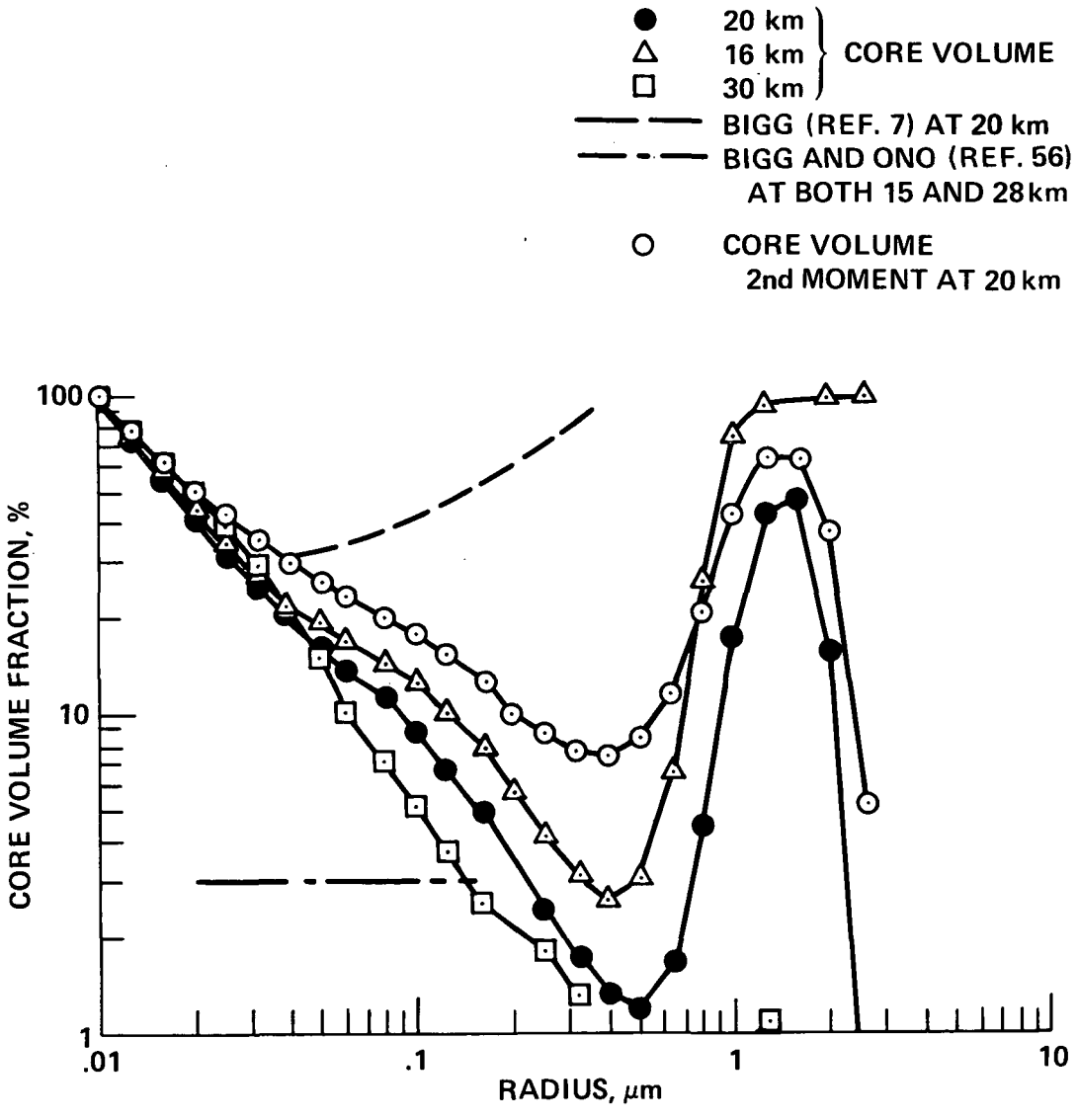

Figure 13.– The average fractional volume of the acid aerosol that is composed of core material as a function of particle size for the reference model calculation and for several different altitudes. Also shown are the second moment of the core volume fraction at 20 km, and two related observations of the core volume fraction.

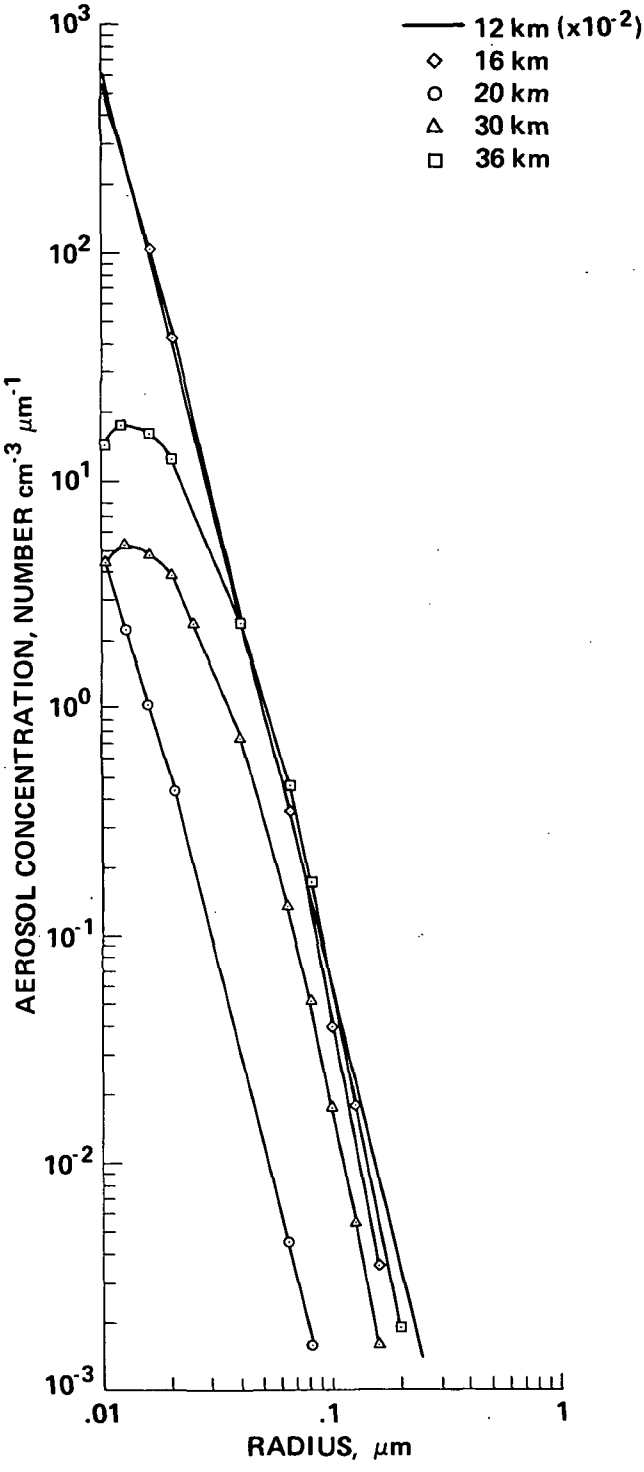

Figure 14.– Reference model calculations of the size distribution of the "unnucleated" core particles below and above the stratospheric aerosol layer (at 12 and 36 km) and embedded within the layer (at 16, 20, and 30 km). The concentration at 12 km has been reduced by 10^{-2} for clarity.

1. Report No.	2. Government Accession No.	3. Recipient's Catalog No.
NASA TP-1363		

4. Title and Subtitle	5. Report Date
THE NASA-AMES RESEARCH CENTER STRATOSPHERIC AEROSOL MODEL. II. SENSITIVITY STUDIES AND COMPARISON WITH OBSERVATIONS	April 1979
	6. Performing Organization Code

7. Author(s)	8. Performing Organization Report No.
O. B. Toon,* R. P. Turco,† P. Hamill,* C. S. Kiang,‡ and R. C. Whitten*	A-7551
	10. Work Unit No. 198-30-02

9. Performing Organization Name and Address	11. Contract or Grant No.
*NASA-Ames Research Center, Moffett Field, Calif. 94035 †R & D Associates, Marina del Rey, Calif. 90291 ‡National Center for Atmospheric Research, Boulder, Colo. 80303	
	13. Type of Report and Period Covered: Technical Paper

12. Sponsoring Agency Name and Address	14. Sponsoring Agency Code
National Aeronautics and Space Administration Washington, D. C. 20546	

15. Supplementary Notes

16. Abstract

We have performed sensitivity tests on a one-dimensional, physical-chemical model of the unperturbed stratospheric aerosols and have compared model calculations with observations. The tests and comparisons suggest that coagulation controls the particle number mixing ratio, although the number of condensation nuclei at the tropopause and the diffusion coefficient at high altitudes are also important. The sulfate mass and large particle number ($r > 0.15$ μm) mixing ratios are controlled by growth, sedimentation, evaporation at high altitudes, and washout below the tropopause. The sulfur gas source strength and the aerosol residence time are much more important than the supply of condensation nuclei in establishing mass and large particle concentrations. The particle size is also controlled mainly by gas supply and residence time. OCS diffusion (not SO_2 diffusion) dominates the production of stratospheric H_2SO_4 particles during unperturbed times, although direct injection of SO_2 into the stratosphere could be significant if it normally occurs regularly by some transport mechanism. We suggest a number of *in situ* observations of the aerosols and laboratory measurements of aerosol parameters that can provide further information about the physics and chemistry of the stratosphere and the aerosols found there.

17. Key Words (Suggested by Author(s))	18. Distribution Statement
Stratosphere Pollution Aerosol Atmosphere modeling	Unlimited STAR Category – 47

19. Security Classif. (of this report)	20. Security Classif. (of this page)	21. No. of Pages	22. Price*
Unclassified	Unclassified	69	$4.50

*For sale by the National Technical Information Service, Springfield, Virginia 22161

NASA-Langley, 1979

National Aeronautics and
Space Administration

Washington, D.C.
20546

Official Business
Penalty for Private Use, $300

THIRD-CLASS BULK RATE

Postage and Fees Paid
National Aeronautics and
Space Administration
NASA-451

NASA

POSTMASTER: If Undeliverable (Section 158 Postal Manual) Do Not Return